Introduction to integral equations for time harmonic acoustic scattering problems

Xavier ANTOINE*†

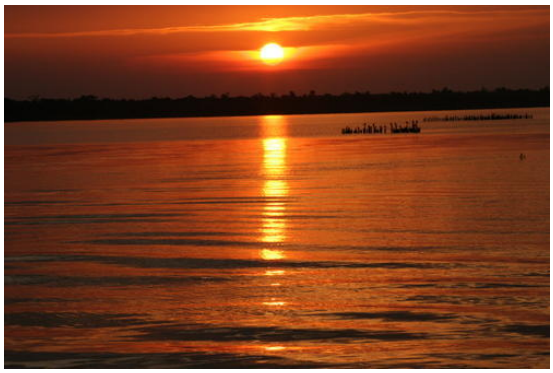

*Institut Elie Cartan Nancy (IECN), Université de Lorraine, Bureau 301, B.P. 239, F-54506 Vandoeuvre-lès-Nancy Cedex, FRANCE. *E-mail*: xavier.antoine@univ-lorraine.fr
Url: X. ANTOINE Homepage

†Scattering of waves: beautiful sunshine illuminating Maracaïbo lake, Puerto Concha, Venezuelan Andes.

Contents

1 Introduction

This course presents some lecture notes given at the CIMPA Research school on Mathematical Modeling and Numerical Simulation at Simon Bolivar University, Caracas, Venezuela, in april 2012. The aim is to give some elements on the theoretical and numerical developments of integral equation formulations for time harmonic acoustic scattering problems.

Wave scattering in the time harmonic regime is known to be an extremely active and difficult area of research with many possible applications in civil and military domains. The applications can require different physics related to wave scattering: acoustics, electromagnetic, elasticity. Applications can be of different natures: radar, sonar, aerospace and aeronautics design, medical imaging, underwater acoustics, diffraction gratings, optics... Therefore, this is a huge area with very exciting applications that need top level computational developments and emerging new ideas to solve the most advanced challenging problems. In particular, high frequency scattering remains an unsolved numerical problem with many applications. To illustrate these motivations, Figure 1 presents images where scattering of waves is the main phenomena. Therefore, you can see that you can meet this topic everyday and everywhere, from small (nano photonics for example) to large (astronomy) scales problems.

Figure 1: Where wave scattering can be met.

An example of application which requires very powerful numerical methods for the prediction of scattering phenomena is given on Figure 2. We can indeed see the surface electromagnetic field created on an aircraft by an incident wave field. This can be useful when for example you investigate ElectroMagnetic Compatibility (EMC) problems where electromagnetic waves can penetrate inside the aircraft and badly damage its electronic components. This is of first importance for aerospace companies for security reasons and prevention of accidents (but also for costs reduction)!

Considering such a problem is clearly extremely difficult and then numerical methods provide a good understanding of the physical problems at low cost. Another example in aeronautics is related to the control of noise generation when the aircraft lands near a town, therefore creating noise pollution and problems near airports since (hopefully) restrictive administration rules must (are expected to?) be followed by the aircraft companies.

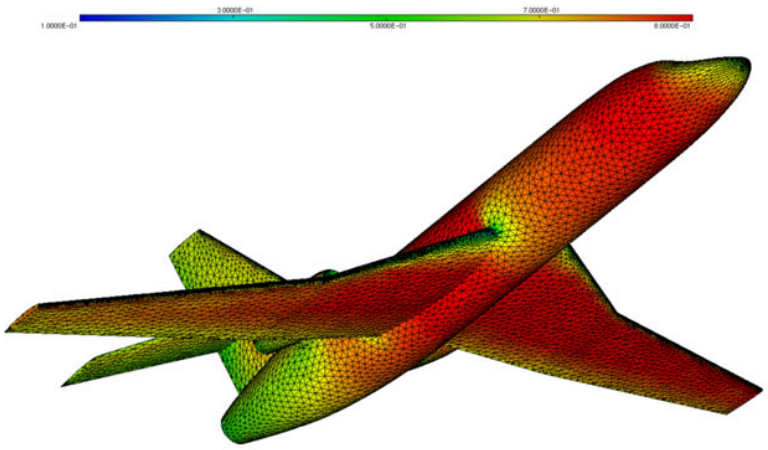

Figure 2: An example of electromagnetic surface field computed through integral equations

One common difficult point to all these problems is that they are set in an unbounded domain making the design of a suitable and accurate numerical method very challenging. Different directions exist. I will develop here mainly the method of integral equation formulations. A first section gives some general notions about wave propagation and introduces the scattering problem. A second section provides the basic elements for understanding integral equation formulations and writing the most standard integral equations to solve. A last section is devoted to present the full strategy for solving these integral equations and a conclusion.

I expect that you will enjoy the trip, oscillating between physics, mathematics and numerics...

If people do not believe that mathematics is simple,
it is only because they do not realize how complicated life is.

J.Von Neumann

2 Basic equations in acoustics scattering

2.1 The one-dimensional case

In the one-dimensional case, the wave equation writes

$$\partial_x^2 U - \frac{1}{c^2}\partial_t^2 U = -Q\delta_{x_Q} \tag{1}$$

in $\mathbb{R}_x \times]0;T]$, where $U = U(x,t)$ is the perturbed acoustic pressure, x is the spatial coordinate and t is the time variable. We consider a constant sound speed c for the homogeneous[1] isotropic[2] medium $\mathbb{R}_x$. The source is considered as a point source with amplitude Q, located at point x_Q. The free-space solutions (that is for $Q = 0$) of Eq. (1) can be written as the sum of a left and a right traveling waves (φ and ψ, respectively here, see Figure 3) if we assume that the initial data U_0 and U_1 are compactly supported in a domain $]-R;R[$. More precisely, if we have (for $c = 1$)

$$\begin{cases} \partial_x^2 U - \partial_t^2 U = 0, (x,t) \in \mathbb{R}_x \times]0;T[, \\ U(x,0) = U_0(x), x \in \mathbb{R}_x \\ \partial_t U(x,0) = U_1(x), x \in \mathbb{R}_x, \end{cases} \tag{2}$$

under the assumption that $\mathrm{supp}(U_{0,1}) \subset B(0,R)$ (the ball centered at the origin with radius R), then the solution U can be written as

$$\begin{array}{ccccc} & & U(x,t) = & & \\ \varphi(x+t) & & + & & \psi(x-t) \end{array} \tag{3}$$

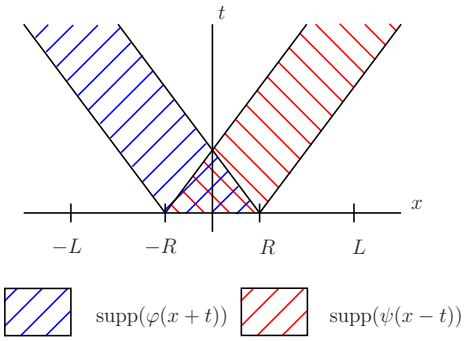

Figure 3: Left and right traveling waves.

Some calculations show that we have

$$U(x,t) = \frac{1}{2}(U_0(x+t) + U_0(x-t)) + \frac{1}{2}\int_{x-t}^{x+t} U_1(y)dy, \tag{4}$$

[1] A medium is homogeneous (or uniform) if its physical properties are unchanged at different points.
[2] Isotropy is uniformity in all orientations.

that is

$$\begin{cases} 2\varphi(x) = U_0(x) + \displaystyle\int_{-\infty}^{x} U_1(y)dy, \\ 2\psi(x) = U_0(x) - \displaystyle\int_{-\infty}^{x} U_1(y)dy. \end{cases} \tag{5}$$

Let us remark that, for $|x|$ sufficiently large, that is $\forall x$ such that $|x| > L$, the supports of the two wavefields φ and ψ are disjoints. This implies e.g. that for $x = -L$, we have: $U(x,t) = \varphi(x+t)$, and so $\partial_x U = \partial_t U$. In a symmetrical way, we have for the right traveling wave: $x = L$, and $U(x,t) = \psi(x-t)$, and so $\partial_x U = -\partial_t U$. By introducing the outwardly directed unit normal vector $\boldsymbol{n}$ to $]-L;L[$, we have the unification of the two boundary conditions

$$\partial_{\boldsymbol{n}} U + \partial_t U = 0, \tag{6}$$

at $x = \pm L$. This means that, if one wants to solve numerically the initial value problem, which is a difficult task since it is set in an unbounded domain $\mathbb{R}_x$, we may rather consider to solve the following Initial Boundary Value Problem (IBVP): find the approximate field U^a such that

$$\begin{cases} \partial_x^2 U^a - \partial_t^2 U^a = 0, (x,t) \in \Omega \times]0;T[, \\ U^a(x,0) = U_0^a(x), x \in \Omega, \\ \partial_t U^a(x,0) = U_1^a(x), x \in \Omega, \\ \partial_{\boldsymbol{n}} U^a + \partial_t U^a = 0, (x,t) \in \{-L;L\} \times]0;T], \end{cases} \tag{7}$$

which is set in a bounded spatial domain, that is $\Omega =]-L;L[$. The main point here is that numerically computing U^a in Ω requires a finite number of grid points unlike working in $\mathbb{R}_x$. Furthermore, in the special case of a one-dimensional problem with constant wave speed, we can prove that we have: $U^a(x,t) = U_{|\Omega}(x,t)$ in $\Omega \times]0;T]$ which means that the restriction of the solution U of the initial system exactly coincides with the solution U^a to the bounded domain problem. Therefore, the two waves travel through the boundaries $\Gamma := \{-L;L\}$ without being reflected back into the domain as the physics does. For this reason, the boundary condition Eq. (6) is said to be a Transparent Boundary Condition (TBC). Let us also remark that deriving the TBC can be done by using Laplace transform (that in some sense leads to working in the frequency domain as done later for time harmonic waves).

2.2 Going to higher dimensions

Let us now come to the two- and three-dimensional cases by considering the wave equation

$$\Delta U - \frac{1}{c^2}\partial_t^2 U + Q\delta_{\boldsymbol{x}_Q} = 0, \qquad \forall \boldsymbol{x} \in \Omega^+. \tag{8}$$

For an easy reading, the vectors will be bold typed. The spatial variable is denoted by $\boldsymbol{x} = (x_1, ..., x_d)$, for $d = 2, 3$. The Laplace operator is $\Delta = \sum_{j=1}^{d} \partial_{x_j}^2$. The domain Ω^+ is supposed to be unbounded, isotropic and homogeneous. This domain can be

(like in the next Sections) the complementary set of a bounded (open set) scatterer Ω^-. Time harmonic waves consists in writing the point source with $Q = \widetilde{Q}e^{-\iota\omega t}$ and the solutions to the wave equation

$$U(\boldsymbol{x}, t) = u(\boldsymbol{x})e^{-\iota\omega t}. \tag{9}$$

The real valued parameter ω is called the pulsation of the wave. The unknown u is the complex pressure field and $\iota := \sqrt{-1}$ is the complex unit. By substitution of the two above expressions into the wave equation (8), one gets

$$\Delta u + \frac{\omega^2}{c^2}u + \widetilde{Q}\delta_{\boldsymbol{x}_Q} = 0, \forall \boldsymbol{x} \in \Omega^+, \tag{10}$$

which is more commonly rewritten as

$$\Delta u + k^2 u + \widetilde{Q}\delta_{\boldsymbol{x}_Q} = 0, \forall \boldsymbol{x} \in \Omega^+. \tag{11}$$

The operator $\Delta + k^2$ is called the Helmholtz[3] operator.

Figure 4: Hermann Ludwig Ferdinand Von Helmholtz (1821-1894).

We also introduce the following physical quantities

$$\begin{aligned} &\text{frequency} : f := \frac{\omega}{2\pi}, \\ &\text{wavelength} : \lambda := \frac{2\pi}{k} = \frac{c}{f} = \frac{2\pi c}{\omega}(ms^{-1}s = m). \end{aligned} \tag{12}$$

The sound speed is yet a constant. For example, the value of the speed of sound in the air at temperature 20 degrees Celsius is $324\ ms^{-1}$.

Since we are dealing with a boundary value problem, one must impose a boundary condition on the boundary Γ of $\Omega^+ := \mathbb{R}^d/\overline{\Omega^-}$. Different kinds of boundary conditions can be considered. A first possibility is to fix the Dirichlet[4] boundary condition

$$u := u^{\text{imposed}}, \text{on } \Gamma, \tag{13}$$

[3]Hermann Ludwig Ferdinand Von Helmholtz (1821-1894), was a German physicist.

[4]Johann Peter Gustav Lejeune Dirichlet (1805-1859) was a German mathematician.

where we prescribe the value of the field at the interface Γ. This boundary condition is also referred to as *sound soft* body boundary condition.

Figure 5: Johann Peter Gustav Lejeune Dirichlet (1805-1859).

Another possibility is to impose the value of the normal velocity field

$$\partial_{\boldsymbol{n}} u := \nabla u \cdot \boldsymbol{n} := \iota\rho\omega \mathrm{v}_{\boldsymbol{n}}^{\text{imposed}}. \tag{14}$$

This inhomogeneous Neumann[5] boundary condition is also called *sound hard body* boundary condition in the acoustics literature.

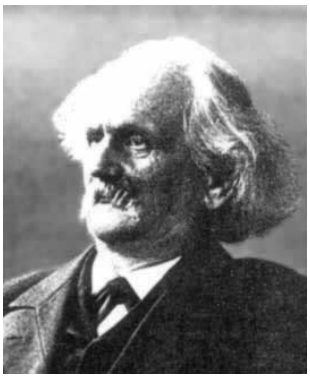

Figure 6: Carl Gottfried Neumann (1832-1925).

In practice, the imposed surface field is given through the expression of the incident (plane) wave field (see the next sections). As a remark, let us also note that other more complex boundary conditions can be met as the impedance (Fourier[6]-Robin[7]) boundary condition

$$\partial_{\boldsymbol{n}} u + \alpha u := g,$$

[5]Carl Gottfried Neumann (1832-1925) was a German mathematician.
[6]Jean Baptiste Joseph Fourier (1768-1830) was a French mathematician and physicist.
[7]Victor Gustave Robin (1855-1897) was also a French mathematician.

where, g is a given function and α is a complex-valued function, or even the generalized impedance boundary condition

$$\partial_{\boldsymbol{n}} u + \alpha u + \beta \Delta_\Gamma u := g,$$

if we define by Δ_Γ the Laplace[8]-Beltrami[9] operator over the surface Γ and by β a complex-valued function on Γ. Let us remark also that for physical reasons the functions α and β are required to satisfy certain (positivity) properties (that we do not develop here) for well-posedness of the boundary value problem. Finally, if one wants to represent the field in the time domain then we have to use the expression (9).

We now specifically consider the time harmonic scattering problem. More precisely, the problem is the following. We consider a time harmonic incident wave u^{inc} that highlights a bounded obstacle Ω^- with surface Γ (for example the submarine presented in Figure 7).

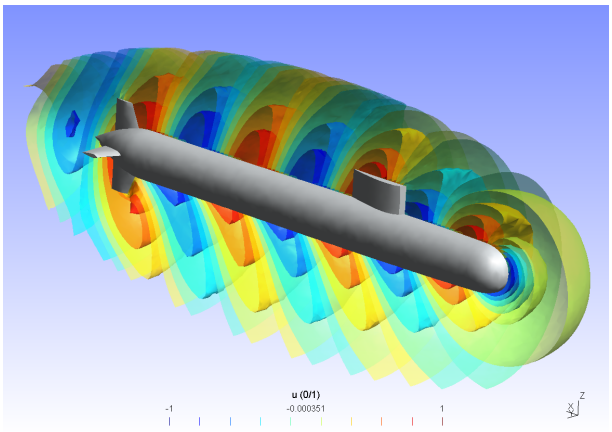

Figure 7: Scattering by a model submarine (by using a volumetric formulation, finite element methods, an artificial boundary condition and a domain decomposition algorithm).

We want to compute the scattered field u solution to

$$\left\{ \begin{array}{l} \Delta u + k^2 u = 0, \text{ in } \Omega^+, \\ u := -u^{\text{inc}}, \text{ on } \Gamma, \end{array} \right. \tag{15}$$

which is a boundary value problem set in an *unbounded domain*. What is really the problem now? Can we solve it? The answer is no because there is no uniqueness of the solution.

Indeed, let us come back to the one-dimensional example. Let us consider that we want to solve

$$\left\{ \begin{array}{l} \partial_x^2 u + k^2 u = 0, \text{ in } \Omega^+ :=]0; +\infty[, \\ u := 1, \text{ at } x = 0. \end{array} \right. \tag{16}$$

[8]Pierre-Simon de Laplace (1749-1827) was French mathematician, astronom and physicist.
[9]Eugenio Beltrami (1835-1899) was an Italian mathematician

Then, the solution writes down

$$u = A^+ e^{\iota kx} + A^- e^{-\iota kx}, \tag{17}$$

where $A^\pm$ are two complex valued coefficients to determine. If one uses the boundary condition, these constants must fullfil

$$A^+ + A^- = 1. \tag{18}$$

But we see that it is not enough to conclude. The system is overdetermined. This means that one (boundary?) condition is missed. Let us consider now that, at a given point in the exterior domain $]0; +\infty[$, we impose the transparent boundary condition derived before in the time domain. In the harmonic regime, one has

$$\partial_{\boldsymbol{n}} U + \frac{1}{c}\partial_t U = \partial_{\boldsymbol{n}} u - \iota\frac{\omega}{c}u = \partial_{\boldsymbol{n}} u - \iota k u = 0. \tag{19}$$

Then, by using (17), this implies that

$$A^+(\iota k - \iota k) + A^-(-\iota k - \iota k) = 0, \tag{20}$$

that is: $-2\iota k A^- = 0$, or $A^- = 0$. Together with Eq. (18), one can conclude that: $A^+ = 1$ and so that

$$u = e^{\iota kx}. \tag{21}$$

This means that, by adding the transparent boundary condition (19), we have been able to get the uniqueness of the solution to the boundary value problem (16). The boundary condition acted as a filter in the frequency regime so that we can select the outgoing wave $e^{\iota kx}$ traveling to the right and filtering the incoming wave $e^{-\iota kx}$ going to the left. This boundary condition is of course at finite distance but translates the expected behavior of the solution at infinity.

For higher dimensions, a suitable condition at infinity has been introduced in 1912 by Sommerfeld[10] in order to precise the asymptotic behavior of the solution.

More precisely, in the three-dimensional setting, the so-called Sommerfeld radiation condition at infinity writes

$$\lim_{R^\infty \to +\infty} R^\infty |\partial_{R^\infty} u - \iota k u| = 0, \tag{22}$$

uniformly in all directions. This physically means that the energy disturbances by the structure should die at infinity. Mathematically, this provides the uniqueness of the solution. In the d-dimensional setting, one must take care to the fact that the Sommerfeld condition depends on d. Indeed, the condition writes down

$$\lim_{||\boldsymbol{x}|| \to +\infty} ||\boldsymbol{x}||^{(d-1)/2}(\nabla u \cdot \frac{\boldsymbol{x}}{||\boldsymbol{x}||} - \iota k u) = 0, \tag{23}$$

uniformly in all directions. This last equation completes system (15) leading to a well-posed scattering boundary value problem.

[10] Arnold Sommerfeld (1868-1951) was a German physicist.

Figure 8: Arnold Sommerfeld (1868-1951) (photo from 1897).

2.3 An exact solution for single scattering: the disk case

When one wishes to develop some numerical methods, one must be able to have some benchmark solutions. One possibility is to consider simple scattering geometries in the two- and three-dimensional cases. The goal of this section is to precise the case of one single disk, multiple scattering configurations being harder to treat.

Let us consider a single disk centered at the origin and with radius R. The polar coordinates system is designated by (r, θ). We consider an incident plane wave u^{inc} defined by

$$u^{\text{inc}} := e^{\iota \mathbf{k} \cdot \boldsymbol{x}}, \tag{24}$$

where the vector wavenumber $\mathbf{k}$ is defined by

$$\mathbf{k} := k(\cos(\theta^{\text{inc}}), \sin(\theta^{\text{inc}}))^T. \tag{25}$$

The angle of incidence θ^{inc} is given in the polar system. Plane waves are standard physically admissible incident wave fields that are used in practice. In the polar coordinates system, we then have

$$\begin{aligned} u^{\text{inc}} := e^{\iota k(x_1 \cos(\theta^{\text{inc}}) + x_2 \sin(\theta^{\text{inc}}))} &= e^{\iota k r(\cos(\theta)\cos(\theta^{\text{inc}}) + \sin(\theta)\sin(\theta^{\text{inc}}))} \\ &= e^{\iota k r \cos(\theta - \theta^{\text{inc}})}, \end{aligned} \tag{26}$$

by using standard trigonometric formulae. To go further into the derivation of the exact solution, one must use the following proposition.

Proposition 1. *We have the Jacobi*[11] *expansion*

$$e^{\iota w \cos\varphi} = \sum_{n \in \mathbb{Z}} (-\iota)^n J_n(w) e^{\iota n \varphi}, \tag{27}$$

[11] Carl Gustav Jacob Jacobi (1804-1851) was a German mathematician.

where J_n are the Bessel[12] special functions of the first kind.

The first kind Bessel functions $J_\alpha(x)$ are the solutions to the following differential equation

$$x^2\frac{d^2}{dx^2}y + x\frac{d}{dx}y + (x^2 - \alpha^2)y = 0, \tag{28}$$

that are finite are the origin. These functions naturally arise here because of the particular cylindrical geometry of our problem. Indeed, the Helmholtz operator in the polar coordinates system is given by

$$\Delta + k^2 := \partial_r^2 + \frac{1}{r}\partial_r + \frac{1}{r^2}\partial_\theta^2 + k^2. \tag{29}$$

So, this means that if one looks for the Fourier series expansion of the solution as

$$u(r,\theta) = \sum_{m\in\mathbb{Z}} u_m(r)e^{\iota m\theta}, \tag{30}$$

then the coefficients u_m are the smooth functions solutions to

$$(r^2\partial_r^2 + r\partial_r + (k^2 - m^2))u_m = 0. \tag{31}$$

This gives that $u_m(r) = J_m(kr)$. The singular solutions at the origin of (28) are the Bessel functions of the second kind, Y_α, which are also called Neumann functions. These are given by $Y_m(kr)$ in our situation. Finally, our incident wave writes

$$u^{\text{inc}}(r,\theta) = \sum_{n\in\mathbb{Z}}(-\iota)^n J_n(kr)e^{\iota n(\theta-\theta^{\text{inc}})} \tag{32}$$

by using the Equations (26) and (27). Figures 9 report the graphs of the Bessel functions J_n and Y_n to illustrate our discussion.

Then, one wants to compute the solution to the Helmholtz equation in the polar coordinates system. The scattered field is given by

$$u(r,\theta) = \sum_{n\in\mathbb{Z}} A_n^+ H_n^{(1)}(kr)e^{\iota n\theta} + A_n^- H_n^{(2)}(kr)e^{\iota n\theta}, \tag{33}$$

where we consider that $\theta^{\text{inc}} = 0$. This last assumption is not restriction since our problem has cylindrical symmetry. The new special functions $H_n^{(1)}$ and $H_n^{(2)}$ are respectively called the Hankel[13] function of the first- and second-kind of order n (sometimes also called third order Bessel functions). They are defined by

$$\begin{cases} H_\alpha^{(1)}(x) := J_\alpha(x) + \iota Y_\alpha(x), \\ H_\alpha^{(2)}(x) := J_\alpha(x) - \iota Y_\alpha(x). \end{cases} \tag{34}$$

[12]Introduced by Daniel Bernoulli (1700-1782) (Swiss mathematician) and generalized by Friedrich Bessel (German mathematician, (1784-1846)).

[13]Hermann Hankel (1839-1873) was a German mathematician.

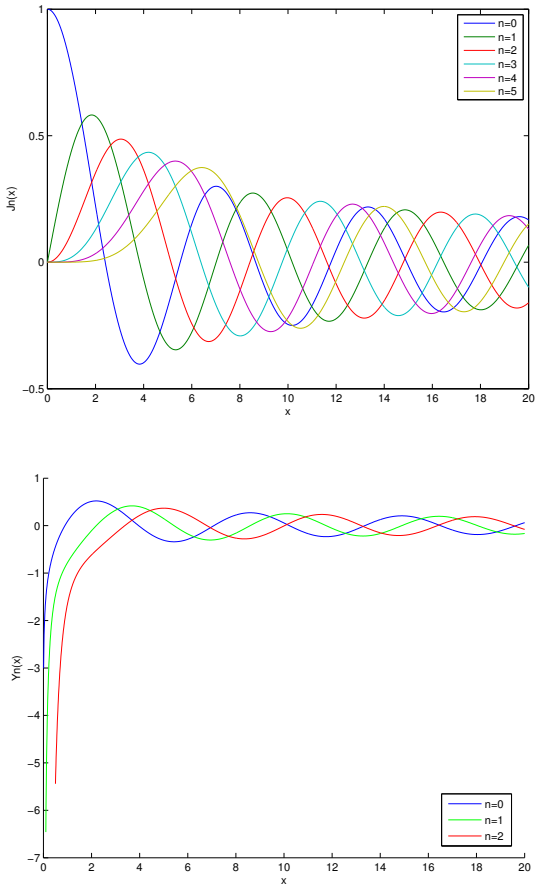

Figure 9: Special Bessel functions $J_n(x)$ and $Y_n(x)$ for different values of x and n (computed with Matlab functions `besselj` and `bessely`). Note the singularity or not at the origin and the decay of the functions for large x arguments. Oscillations are also present which translate the property that we are considering wave like problems.

If one uses the Dirichlet boundary condition, by separation of variables, one obtains

$$A_n^+ H_n^{(1)}(kR) + A_n^- H_n^{(2)}(kR) = -(-\imath)^n J_n(kR) \tag{35}$$

on the scatterer surface. Some asymptotic expansions allow however to show that the outgoing modes are related to the functions $H_n^{(1)}$ while $H_n^{(2)}$ transports the incoming modes. Because of the Sommerfeld radiation condition at infinity which tells that the solution is outgoing, one has to fix: $A_n^- = 0$, for all $n \in \mathbb{Z}$. You have to notice here that this is very similar to the one-dimensional case. Finally, by using (35), one can conclude that

$$A_n^+ = -(-\imath)^n \frac{J_n(kR)}{H_n^{(1)}(kR)} \tag{36}$$

and that the exact solution can be written as

$$u(r,\theta) = -\sum_{n\in\mathbb{Z}} (-\iota)^n \frac{J_n(kR)}{H_n^{(1)}(kR)} H_n^{(1)}(kr) e^{\iota n\theta} \tag{37}$$

for $r \geq R$. Very similar calculations lead to the expression of the exact solution for the Neumann boundary condition on a disk and an incident plane wave. This solution is also often called Mie[14] series expansion. One gets

$$u(r,\theta) = -\sum_{n\in\mathbb{Z}} (-\iota)^n \frac{J_n'(kR)}{H_n^{(1)'}(kR)} H_n^{(1)}(kr) e^{\iota n\theta}, \tag{38}$$

where the prime $'$ means that we consider the derivative of the function thanks to its argument. The strategy also applies to impedance and generalized impedance boundary conditions.

In the three-dimensional case, an approach based on spherical harmonics functions can be developed. The calculations are longer and can be found in reference textbooks about acoustics. Let us remark that plane waves are then written as (24) but with

$$\mathbf{k} := k(\cos(\theta^{\text{inc}})\sin(\phi^{\text{inc}}), \sin(\theta^{\text{inc}})\sin(\phi^{\text{inc}}), \cos(\phi^{\text{inc}}))^T. \tag{39}$$

3 Potential theory - integral equations

In this section, we present how to solve an exterior boundary value problem set in an unbounded computational domain *via* the integral equations method. First, we recall the basic acoustic scattering problem and some notations. Next, we give elements of potential theory that are crucial for the integral equation method. Finally, we discuss the derivation of the classical direct and indirect integral equations for both Dirichlet and Neumann boundary conditions.

3.1 Acoustic scattering problems

Let us define a d-dimensional bounded domain $\Omega^- \subset \mathbb{R}^d$ representing an impenetrable body with boundary $\Gamma := \partial\Omega^-$. We denote by $\Omega^+ := \mathbb{R}^d \setminus \overline{\Omega^-}$ the associated homogeneous exterior domain of propagation. Consider the scattering of an incident time-harmonic acoustic wave u^{inc} by the obstacle Ω^-. The scattered field u^+ satisfies the following exterior boundary-value problem

$$\begin{cases} \Delta u^+ + k^2 u^+ = 0, \ \text{ in } \Omega^+, \\ u^+|_\Gamma = -u^{\text{inc}}|_\Gamma \text{ or } \partial_{\boldsymbol{n}} u^+|_\Gamma = -\partial_{\boldsymbol{n}} u^{\text{inc}}|_\Gamma, \ \text{ on } \Gamma, \\ \lim\limits_{\|\boldsymbol{x}\|\to+\infty} \|\boldsymbol{x}\|^{(d-1)/2}(\nabla u^+ \cdot \dfrac{\boldsymbol{x}}{\|\boldsymbol{x}\|} - \iota k u^+) = 0, \end{cases} \tag{40}$$

Figure 10 is a schematic representation of the problem.

[14] Gustav Adolf Feodor Wilhelm Ludwig Mie (1869-1957) was a German physicist.

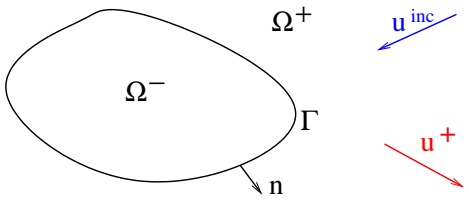

Figure 10: Scattering problem configuration.

Let us introduce the functional Sobolev[15] spaces [43]

$$
\begin{array}{l}
H^s_{\mathrm{loc}}(\overline{\Omega^+}) := \left\{ v \in \mathcal{D}'(\Omega^+) / \psi v \in H^s(\Omega^+), \forall \psi \in \mathcal{D}(\mathbb{R}^d) \right\}, \quad s \geq 1, \\
H^1_-(\Delta) := H^1(\Delta, \overline{\Omega^-}) := \left\{ u \in H^1(\overline{\Omega^-}); \Delta u \in L^2(\overline{\Omega^-}) \right\}, \\
H^1_+(\Delta) := H^1_{\mathrm{loc}}(\Delta, \overline{\Omega^+}) := \left\{ u \in H^1_{\mathrm{loc}}(\overline{\Omega^+}); \Delta u \in L^2_{\mathrm{loc}}(\overline{\Omega^+}) \right\}.
\end{array}
$$

For $u \in H^1_\pm(\Delta)$, the exterior $(+)$ and interior $(-)$ trace operators of order j ($j = 0$ or 1) can be defined by

$$
\begin{array}{rcl}
\gamma_j^\pm : H^1_\pm(\Delta) & \to & H^{1/2-j}(\Gamma) \\
u & \mapsto & \gamma_j^\pm u^\pm = \partial_{\boldsymbol{n}}^j u^\pm|_\Gamma.
\end{array}
\tag{41}
$$

In this functional setting, the existence and uniqueness of the solution to the scattering problem

$$
\left\{
\begin{array}{l}
\text{Find } u^+ \in H^1_{\mathrm{loc}}(\overline{\Omega^+}) \text{ such that} \\
\Delta u^+ + k^2 u^+ = 0, \ \text{ in } \mathcal{D}'(\Omega^+), \\
\gamma_j^+ u^+ = g := -\gamma_j^+ u^{\mathrm{inc}}, \quad \text{in } H^{1/2-j}(\Gamma), \quad \text{for } j = 0 \text{ or } 1, \\
\lim\limits_{\|\boldsymbol{x}\| \to +\infty} \|\boldsymbol{x}\|^{(d-1)/2} (\nabla u^+ \cdot \dfrac{\boldsymbol{x}}{\|\boldsymbol{x}\|} - \iota k u^+) = 0,
\end{array}
\right.
\tag{42}
$$

can be proved [27].

The first main difficulty arising in the numerical solution of the exterior boundary-value problem (42) is related to the unboundedness of the computational domain Ω^+. A solution is to apply the integral equations method [23, 27]. This approach allows to reformulate the initial boundary-value problem as an integral equation defined on the boundary Γ of the scattering obstacle Ω^-. Then, this method reduces the dimension of the problem to $d - 1$. Boundary integral equations are derived from potential theory. Let us give in the some elements of this theory but before this, we need to introduce the notion of fundamental solution.

3.2 Fundamental solution for the acoustic scattering problem

The aim here is to compute the response of a point source, that is the Green[16] function, placed at a point $\boldsymbol{x}$ to a point $\boldsymbol{y}$. We denote this fundamental solution for these two

[15] Sergueï Lvovitch Sobolev (1908-1989) was a Russian mathematician and physicist.
[16] George Green (1793-1841) is an American mathematician.

points by $G(\boldsymbol{x}, \boldsymbol{y})$. It satisfies the following equation

$$-(\Delta_{\boldsymbol{x}} G + k^2 G) = \delta(\boldsymbol{x}, \boldsymbol{y}), \tag{43}$$

where δ is again the delta Dirac distribution. It is expected that G is spherical for the three-dimensional case (and radial for the two-dimensional problem) since it must scattered uniformly in all directions. Let us first consider the spherical form of the Helmholtz equation for a (θ, ϕ)-independent function (spherical symmetry)

$$\Delta\phi = (\partial_r^2 + \frac{2}{r}\partial_r)\phi = \frac{1}{r}\frac{d^2}{dr^2}(r\phi). \tag{44}$$

Then, the spherical solution to the Helmholtz equation can be written as the solution to

$$\frac{d^2}{dr^2}(r\phi) + k^2(r\phi) = 0 \tag{45}$$

that is

$$\phi = \frac{1}{r}(A^+ e^{\iota kr} + A^- e^{-\iota kr}). \tag{46}$$

Since the solution is required to be outgoing, then one gets that: $A^- = 0$. Therefore, we are looking at the Green's function under the form

$$G(\boldsymbol{x}, \boldsymbol{y}) = A\frac{e^{\iota kr}}{r} \tag{47}$$

with $r = ||\boldsymbol{x} - \boldsymbol{y}||$ and A is a constant to determine. To this end, let us consider a small spherical domain S_ε enclosing the origin (when there is a singularity assuming that $\boldsymbol{x} = \boldsymbol{0}$). Then, we formally have

$$\int_{S_\varepsilon} (\Delta + k^2) G dS_\varepsilon(\boldsymbol{y}) = -\int_{S_\varepsilon} \delta_{\boldsymbol{0}} dS_\varepsilon(\boldsymbol{y}) = -1. \tag{48}$$

By using the Gauss theorem, one also obtains that

$$\int_{S_\varepsilon} \Delta G dS_\varepsilon(\boldsymbol{y}) = \int_{\partial S_\varepsilon} \partial_{\boldsymbol{n}(\boldsymbol{y})} d\partial S_\varepsilon(\boldsymbol{y}) = 4\pi A(\iota k\varepsilon - 1)e^{\iota k\varepsilon}. \tag{49}$$

By making use of the spherical coordinates system we have

$$\begin{aligned}\int_{S_\varepsilon} k^2 G dS_\varepsilon(\boldsymbol{y}) = k^2 A \int_0^\varepsilon \int_0^{2\pi} \int_0^\pi \frac{1}{r} e^{\iota kr} r^2 \sin(\varphi) d\varphi d\theta dr \\ = 4\pi A((1 - \iota k\varepsilon)e^{\iota k\varepsilon} - 1).\end{aligned} \tag{50}$$

This finally provides

$$-4\pi A = -1, \tag{51}$$

that is

$$A = \frac{1}{4\pi}. \tag{52}$$

As a conclusion, this formal derivation shown that the Green's function is

$$G(\boldsymbol{x},\boldsymbol{y}) = \frac{e^{\iota kr}}{4\pi r} = \frac{e^{\iota k||\boldsymbol{x}-\boldsymbol{y}||}}{4\pi||\boldsymbol{x}-\boldsymbol{y}||}. \tag{53}$$

Similar calculations can be done for the two-dimensional case, resulting in the Green's function

$$G(\boldsymbol{x},\boldsymbol{y}) = \frac{\iota}{4}H_0^{(1)}(k||\boldsymbol{x}-\boldsymbol{y}||). \tag{54}$$

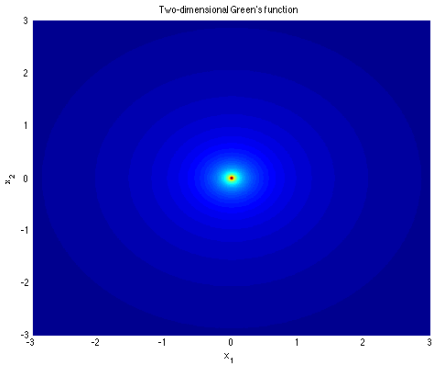

Figure 11: Modulus of the two-dimensional Green's function given by Eq. (54).

Finally, let us remark that a more rigorous derivation of this Green's function can be obtained by using the distributional calculus.

3.3 Potential theory: basic relations - properties

One important point when working with integral equations is that equivalent formulations to the initial scattering problem can be obtained. The essential property is that any solution to the Helmholtz equation can be represented as the linear combination of a single- and a double-layer potentials. The following proposition holds.

Proposition 2. *Let us define the outgoing Green's function G associated with the Helmholtz operator in $\mathbb{R}^d$ by*

$$G(\boldsymbol{x},\boldsymbol{y}) = \begin{cases} \dfrac{\iota}{4}H_0^{(1)}(k\|\boldsymbol{x}-\boldsymbol{y}\|), \text{ for d=2,} \\ \dfrac{1}{4\pi}\dfrac{e^{\iota k\|\boldsymbol{x}-\boldsymbol{y}\|}}{\|\boldsymbol{x}-\boldsymbol{y}\|}, \text{ for d=3,} \end{cases} \tag{55}$$

where $H_0^{(1)}$ designates the first-kind Hankel function of order zero. Let $(v^-, v^+) \in H^1(\Omega^-) \times H^1_{\text{loc}}(\overline{\Omega^+})$ satisfying

$$\Delta v^- + k^2 v^-, \text{ in } \Omega^-,$$

and

$$\begin{cases} \Delta v^+ + k^2 v^+, \ \textit{in } \Omega^+, \\ v^+ \textit{ outgoing wave.} \end{cases}$$

Then, we have

$$L([\partial_{\boldsymbol{n}} v(\boldsymbol{y})]_\Gamma)(\boldsymbol{x}) - D([v(\boldsymbol{y})]_\Gamma)(\boldsymbol{x}) = \begin{cases} v^-(\boldsymbol{x}), \textit{ for } \boldsymbol{x} \in \Omega^-, \\ v^+(\boldsymbol{x}), \textit{ for } \boldsymbol{x} \in \Omega^+, \end{cases} \tag{56}$$

where

$$[v]_\Gamma := \gamma_0^- v^- - \gamma_0^+ v^+, [\partial_{\boldsymbol{n}} v]_\Gamma := \gamma_1^- v^- - \gamma_1^+ v^+,$$

and

$$Lp(\boldsymbol{x}) := \int_\Gamma G(\boldsymbol{x}, \boldsymbol{y}) p(\boldsymbol{y}) d\Gamma(\boldsymbol{y}), \ \ \boldsymbol{x} \notin \Gamma, \tag{57}$$

$$D\phi(\boldsymbol{x}) := \int_\Gamma \partial_{\boldsymbol{n}(\boldsymbol{y})} G(\boldsymbol{x}, \boldsymbol{y}) \phi(\boldsymbol{y}) d\Gamma(\boldsymbol{y}), \ \ \boldsymbol{x} \notin \Gamma, \tag{58}$$

for $(p, \phi) \in H^{1/2}(\Gamma) \times H^{-1/2}(\Gamma)$.

The operators L and D defined above are called the single- and the double-layer potentials respectively. To obtain integral equations set on the boundary Γ, we need the trace formulae for these two potentials (see for instance [43]).

Proposition 3. *The first and second traces on* Γ *of the single-layer and the double-layer potentials are given by*

$$\begin{cases} \gamma_0^- \circ L = \gamma_0^+ \circ L = \mathcal{L} \\ \gamma_1^- \circ L = (\dfrac{\mathcal{I}}{2} + \mathcal{N}) \\ \gamma_1^+ \circ L = (-\dfrac{\mathcal{I}}{2} + \mathcal{N}) \end{cases} \tag{59}$$

and

$$\begin{cases} \gamma_0^- \circ D = (-\dfrac{\mathcal{I}}{2} + \mathcal{D}) \\ \gamma_0^+ \circ D = (\dfrac{\mathcal{I}}{2} + \mathcal{D}) \\ \gamma_1^- \circ D = \gamma_1^+ \circ D = \mathcal{S} \end{cases} \tag{60}$$

where $\mathcal{I}$ *is the identity operator and* $\mathcal{L}, \mathcal{N}, \mathcal{D}$ *and* $\mathcal{S}$ *the four elementary boundary integral operators expressed, for all* $\boldsymbol{x} \in \Gamma$*, by*

$$\begin{aligned} \mathcal{L}p(\boldsymbol{x}) &:= \int_\Gamma G(\boldsymbol{x}, \boldsymbol{y}) p(\boldsymbol{y}) d\Gamma(\boldsymbol{y}) \\ \mathcal{N}p(\boldsymbol{x}) &:= \int_\Gamma \partial_{\boldsymbol{n}(\boldsymbol{x})} G(\boldsymbol{x}, \boldsymbol{y}) p(\boldsymbol{y}) d\Gamma(\boldsymbol{y}) \\ \mathcal{D}\phi(\boldsymbol{x}) &:= \int_\Gamma \partial_{\boldsymbol{n}(\boldsymbol{y})} G(\boldsymbol{x}, \boldsymbol{y}) \phi(\boldsymbol{y}) d\Gamma(\boldsymbol{y}) \\ \mathcal{S}\phi(\boldsymbol{x}) &:= \oint_\Gamma \frac{\partial^2}{\partial \boldsymbol{n}(\boldsymbol{x}) \partial \boldsymbol{n}(\boldsymbol{y})} G(\boldsymbol{x}, \boldsymbol{y}) \phi(\boldsymbol{y}) d\Gamma(\boldsymbol{y}). \end{aligned} \tag{61}$$

Note that the expression defining $\mathcal{S}$ is not an integral (its singularity is not integrable) but a finite part expression associated with a hypersingular kernel and that $\mathcal{N}$ and $\mathcal{D}$ are strongly singular operators which must be understood though the Cauchy[17] Principal Value (CPV) definition. Indeed, if G is given by

$$G(\boldsymbol{x},\boldsymbol{y}) = \frac{1}{4\pi}\frac{e^{\iota k\|\boldsymbol{x}-\boldsymbol{y}\|}}{\|\boldsymbol{x}-\boldsymbol{y}\|}, \text{ for } d=3, \tag{62}$$

then some calculations show that we have

$$\partial_{\boldsymbol{n}(\boldsymbol{x})}G(\boldsymbol{x},\boldsymbol{y}) = \frac{1}{4\pi}\nabla_{\boldsymbol{x}}\frac{e^{\iota k\|\boldsymbol{x}-\boldsymbol{y}\|}}{\|\boldsymbol{x}-\boldsymbol{y}\|}\cdot\boldsymbol{n}(\boldsymbol{x}). \tag{63}$$

But we have that

$$\nabla_{\boldsymbol{x}}\|\boldsymbol{x}-\boldsymbol{y}\| = \frac{\boldsymbol{x}-\boldsymbol{y}}{\|\boldsymbol{x}-\boldsymbol{y}\|}\cdot\boldsymbol{n}(\boldsymbol{x}) \tag{64}$$

leading therefore to

$$\partial_{\boldsymbol{n}(\boldsymbol{x})}G(\boldsymbol{x},\boldsymbol{y}) = \frac{\iota k}{4\pi}\frac{\boldsymbol{x}-\boldsymbol{y}}{\|\boldsymbol{x}-\boldsymbol{y}\|^2}\cdot\boldsymbol{n}(\boldsymbol{x})e^{\iota k\|\boldsymbol{x}-\boldsymbol{y}\|}. \tag{65}$$

A similar but simpler problem if to consider

$$f_2(x) = \int_a^b \frac{1}{y-x}dx, a<x<b,$$

which must be understood in the sense of CPV. Indeed some calculations show that

$$\begin{aligned} f_2(x) &= \lim_{\varepsilon_1\to 0}\int_a^{x-\varepsilon_1}\frac{1}{y-x}dx + \lim_{\varepsilon_2\to 0}\int_{x+\varepsilon_2}^b\frac{1}{y-x}dx \\ &= \log(\frac{b-x}{x-a}) + \lim_{\varepsilon_1\to 0}\log\varepsilon_1 - \lim_{\varepsilon_2\to 0}\log\varepsilon_2 = \log(\frac{b-x}{x-a}) = \text{CPV}(f_2)(x) \end{aligned}$$

if and only if $\varepsilon_1=\varepsilon_2$. The hypersingular character of $\mathcal{S}$ is seen by differentiation. An example of a similar situation is to consider

$$\begin{aligned} f_3(x) = \lim_{\varepsilon\to 0}[\int_a^{x-\varepsilon}\frac{1}{(y-x)^2}dx + \int_{x+\varepsilon}^b\frac{1}{(y-x)^2}dx] \\ = -\frac{1}{x-a} - \frac{1}{b-x} + \lim_{\varepsilon\to 0}\frac{2}{\varepsilon} \end{aligned}$$

which does not even exist in the CPV sense. However, in the integral equation, it is found that the infinite term is cancelled out by

$$\lim_{\varepsilon\to 0}\frac{2}{\varepsilon}\int_{x-\varepsilon}^{x+\varepsilon}\frac{1}{(y-x)^2}dx = \lim_{\varepsilon\to 0} -\frac{2}{\varepsilon}$$

[17] Augustin Louis, baron Cauchy (1789-1857) was a French mathematician.

and therefore the f_3 integral is meaningful in the Hadamard Finite Part (HFP) integral with the finite part given by

$$\mathrm{HPF}(f_3)(x) = -\frac{1}{x-a} - \frac{1}{b-x}.$$

Let us remark that by integration by parts, the weak form of integral equations will only involve singular integrals that can be numerically integrated.

We preferred to keep formally the integral expression for the sake of clarity. Let us now summarize the continuity properties of the elementary boundary integral operators (see for instance [43, Theorem 4.4.1] or Theorems 7.1 and 7.2 in [41]).

Proposition 4. *For a smooth boundary Γ, the boundary integral operators given in Proposition 3 define the following continuous mappings*

$$\begin{array}{rcccl} \mathcal{L} & : & H^s(\Gamma) & \longrightarrow & H^{s+1}(\Gamma), \\ \mathcal{N} & : & H^s(\Gamma) & \longrightarrow & H^s(\Gamma), \\ \mathcal{D} & : & H^s(\Gamma) & \longrightarrow & H^s(\Gamma), \\ \mathcal{S} & : & H^s(\Gamma) & \longrightarrow & H^{s-1}(\Gamma), \end{array} \tag{66}$$

for all $s \in \mathbb{R}$. Moreover, the operators $\mathcal{N}$ and $\mathcal{D}$ are compact from $H^s(\Gamma)$ onto itself for all $s \in \mathbb{R}$.

In the case of a Lipschitz[18] boundary [28, 41], the above continuity properties still hold for $-1 \leq s \leq 0$ (respectively for $0 \leq s \leq 1$) for operators $\mathcal{L}$ and $\mathcal{N}$ (respectively $\mathcal{D}$ and $\mathcal{S}$), while the compactness properties of $\mathcal{N}$ and $\mathcal{D}$ fail. A possible approach to rigorously extend the following developments is to use e.g. some regularizing techniques [18].

The representation (56) allows to determine the near-field around the scatterer. Another physical quantity of interest is the scattering amplitude (or the far-field pattern). For instance, in the two-dimensional case, we have

$$a_0(\boldsymbol{\theta}) = \frac{\iota}{4}\sqrt{\frac{2}{\iota\pi k}} \int_\Gamma e^{-\iota k \boldsymbol{y}\cdot\boldsymbol{\theta}} (\gamma_1^+ u^+(\boldsymbol{y}) + \iota k \boldsymbol{\theta}\cdot\boldsymbol{n}(\boldsymbol{y}) \gamma_0^+ u^+(\boldsymbol{y})) d\Gamma(\boldsymbol{y}).$$

3.4 Standard integral equations formulations

The Helmholtz representation formula (56) leads to the construction of an infinite number of integral equations (equivalent if invertible) in the case of a closed surface. In the case of an open surface, only one integral equation can be written (the EFIE). The aim of this part is to introduce the most standard integral equations for both Dirichlet and Neumann boundary conditions. We usually distinguish between direct and indirect integral equations, each of them having their own mathematical properties.

Let us introduce the following notations

[18] Rudolf Otto Sigismund Lipschitz (1832-1903) was a German mathematician.

- $K_D(\Omega^-) = \{k_m^D, m \in \mathbb{N}\}$, the set of Dirichlet irregular frequencies (interior Dirichlet eigenvalues), is the set of values of k such that the boundary value problem
$$\begin{cases} -\Delta v = k^2 v, & \text{in } \Omega^-, \\ \gamma_0^- v = 0, & \text{on } \Gamma, \end{cases}$$
admits a non vanishing solution.

- $K_N(\Omega^-) = \{k_m^N, m \in \mathbb{N}\}$, the set of Neumann irregular frequencies (interior Neumann eigenvalues), is the set of values of k such that the boundary value problem
$$\begin{cases} -\Delta v = k^2 v, & \text{in } \Omega^-, \\ \gamma_1^- v = 0, & \text{on } \Gamma, \end{cases}$$
admits a non vanishing solution.

3.4.1 The Dirichlet problem: direct integral formulations

The total field w is expressed by $w := u^+ + u^{\text{inc}}$. The direct formulations consist in seeking the total field under the form

$$w(\boldsymbol{x}) = Lp(\boldsymbol{x}) + u^{\text{inc}}(\boldsymbol{x}), \quad \boldsymbol{x} \in \Omega^+. \tag{67}$$

The integral representation (67) ensures that w is solution to the Helmholtz equation in $\Omega^- \cup \Omega^+$, and satisfies the Sommerfeld radiation condition. Then, we have to determine the unknown p such that w satisfies also the Dirichlet boundary condition ($\gamma_0^+ w = 0$). More precisely, the representation (67) corresponds to the particular choice of solutions $(v^-, v^+) := (-u^{\text{inc}}, u^+)$ in Proposition 2, i.e.

$$[v]_\Gamma = 0 \qquad [\partial_{\boldsymbol{n}} v]_\Gamma = -\gamma_1^+ w_{|\Gamma} := p$$

and

$$Lp(\boldsymbol{x}) = \begin{cases} -u^{\text{inc}}(\boldsymbol{x}) & \text{for } \boldsymbol{x} \in \Omega^- \\ u^+(\boldsymbol{x}) & \text{for } \boldsymbol{x} \in \Omega^+. \end{cases} \tag{68}$$

Then, we get the following single-layer potential representation of the total field:

$$Lp(\boldsymbol{x}) + u^{\text{inc}}(\boldsymbol{x}) = \begin{cases} 0 & \text{for } \boldsymbol{x} \in \Omega^- \\ w(\boldsymbol{x}) & \text{for } \boldsymbol{x} \in \Omega^+. \end{cases}$$

Clearly, this formulation is completely equivalent to extending artificially the total field by zero inside Ω^-, which explains that this approach is also referred sometimes to as the *null field method*.

The next step is to obtain an integral equation for the physical unknown $p = -\gamma_1^+ w_{|\Gamma} \in H^{-1/2}(\Gamma)$. To achieve this, the idea is to apply a trace operator to the relation

$$Lp(\boldsymbol{x}) + u^{\text{inc}}(\boldsymbol{x}) = 0, \qquad \forall \boldsymbol{x} \in \Omega^-. \tag{69}$$

At this point, many choices are available. Let us cite three of them leading to classical integral equations of potential theory.

- **EFIE :** This equation is obtained by applying the trace operator γ_0^- to (69). Thanks to the trace relations of Proposition 3, this leads to the well-known Electric Field Integral Equation (EFIE):

$$\mathcal{L}p = -\gamma_0^+ u^{\rm inc}, \quad \text{on } \Gamma. \tag{70}$$

- **MFIE :** This equation is obtained by applying the normal trace operator γ_1^- to (69). Thanks to the trace relations of Proposition 3, this leads to the so-called Magnetic Field Integral Equation (MFIE):

$$(\frac{\mathcal{I}}{2} + \mathcal{N})p = -\gamma_1^+ u^{\rm inc}, \quad \text{on } \Gamma. \tag{71}$$

- **CFIE :** This equation is obtained by applying to (69) the Fourier-Robin (impedance) trace operator $\gamma_1^- + \eta\gamma_0^-$, with $\eta \neq 0$. Once again, the trace relations of Proposition 3 give the Combined Field Integral Equation (CFIE):

$$\left\{(\frac{\mathcal{I}}{2} + \mathcal{N}) + \eta\mathcal{L}\right\} p = -(\gamma_1^+ u^{\rm inc} + \eta\gamma_0^+ u^{\rm inc}), \quad \text{on } \Gamma. \tag{72}$$

The existence and uniqueness results for the above direct integral equations ((70), (71) or (72)) are given in the following theorem.

Theorem 1. *The following properties hold.*

1. *The operator $\mathcal{L}$ defines an isomorphism from $H^{-1/2}(\Gamma)$ onto $H^{1/2}(\Gamma)$ if and only if $k \notin K_D(\Omega^-)$. Under this condition, the EFIE* (70) *is uniquely solvable in $H^{-1/2}(\Gamma)$.*

2. *The operator*
$$(\frac{\mathcal{I}}{2} + \mathcal{N})$$
defines an isomorphism from $H^{-1/2}(\Gamma)$ onto $H^{-1/2}(\Gamma)$ if and only if $k \notin K_N(\Omega^-)$. Under this condition, the MFIE (71) *is uniquely solvable in $H^{-1/2}(\Gamma)$.*

3. *The operator*
$$(\frac{\mathcal{I}}{2} + \mathcal{N}) + \eta\mathcal{L}$$
defines an isomorphism from $H^{-1/2}(\Gamma)$ onto $H^{-1/2}(\Gamma)$ for all $k > 0$ provided $\Im(\eta) \neq 0$ (imaginary part of η). Under this condition, the CFIE (72) *is uniquely solvable in $H^{-1/2}(\Gamma)$ for any frequency $k > 0$.*

In the case where k in an irregular frequency, the integral equations EFIE and MFIE have non zero kernels. Nevertheless, it can be shown that the spurious modes of the EFIE will not radiate in the exterior. Thus, the field is not corrupted outside the object: $\mathcal{L}p = 0$ on $\Gamma \implies Lp = 0$ in Ω^+. Then, the EFIE provides accurate computations and often represents a reference solution. Unlike the EFIE, the spurious solutions of the MFIE do radiate in the exterior domain, leading hence to a wrong solution. Finally, by its construction itself, the CFIE is free of the internal-resonance problem. We consider in the sequel $\eta = -\iota k\alpha/(1-\alpha)$, $\alpha \in]0,1[$,

$$(1-\alpha)\frac{\iota}{k}(\frac{\mathcal{I}}{2}+\mathcal{N})+\alpha\mathcal{L} = -((1-\alpha)\frac{\iota}{k}\gamma_1^+ u^{\text{inc}} + \alpha\gamma_0^+ u^{\text{inc}}), \quad \text{on } \Gamma. \tag{73}$$

A common choice of α for engineering computations is $\alpha = 0.2$ which gives an almost minimal condition number for the CFIE.

3.4.2 The Dirichlet problem: indirect integral formulations

The indirect formulations are based on the assumption that the solution can be expressed in terms of a source density function defined on the boundary. The unknowns are then generally non-physical quantities. The physical variables are solved afterwards in terms of these source densities. Here, we focus on the most commonly used indirect integral formulation independently proposed by Burton-Miller [19] and Brakhage-Werner [13]. The idea is to seek the exterior field as a superposition of the single- and double-layer potentials acting on a fictitious surface density ψ:

$$u^+(\boldsymbol{x}) = (D+\eta L)\psi(\boldsymbol{x}), \quad \forall \boldsymbol{x} \in \Omega^+, \tag{74}$$

where η is a complex-valued coupling parameter to choose. The above expression leads, thanks to the trace relations (3), to the following integral equation :

$$\left\{(\frac{\mathcal{I}}{2}+\mathcal{D})+\eta\mathcal{L}\right\}\psi = -\gamma_0^+ u^{\text{inc}}, \quad \text{on } \Gamma. \tag{75}$$

We consider the above integral equation in the space $H^{1/2}(\Gamma)$ and we can prove the following result.

Theorem 2. *The operator*

$$(\frac{\mathcal{I}}{2}+\mathcal{D})+\eta\mathcal{L}$$

defines an isomorphism from $H^{1/2}(\Gamma)$ onto $H^{1/2}(\Gamma)$ for all $k > 0$ provided $\Im(\eta) \neq 0$. Under this condition, (75) *is uniquely solvable in $H^{1/2}(\Gamma)$ for all frequency $k > 0$.*

This integral equation is uniquely solvable if and only if $\Im(\eta) > 0$. An almost optimal value of η has been obtained in [2, 36, 38] as: $\eta = \iota k$.

3.4.3 The Neumann problem: direct integral formulations

Let us now briefly discuss the derivation of direct integral equations in the case of a Neumann boundary condition. The total field $w := u^+ + u^{\rm inc}$ is sought under the form

$$w(\boldsymbol{x}) = D\phi(\boldsymbol{x}) + u^{\rm inc}(\boldsymbol{x}), \quad \boldsymbol{x} \in \Omega^+. \tag{76}$$

Proposition 2 for $(v^-, v^+) := (-u^{\rm inc}, u^+)$ leads to:

$$[v]_\Gamma = -\gamma_0^+ w := \phi,$$

$$[\partial_{\boldsymbol{n}} v]_\Gamma = 0,$$

and

$$D\phi(\boldsymbol{x}) = \begin{cases} -u^{\rm inc}(\boldsymbol{x}) & \text{for } \boldsymbol{x} \in \Omega^- \\ u^+(\boldsymbol{x}) & \text{for } \boldsymbol{x} \in \Omega^+. \end{cases}$$

Then, we get

$$D\phi(\boldsymbol{x}) + u^{\rm inc}(\boldsymbol{x}) = \begin{cases} 0 & \text{for } \boldsymbol{x} \in \Omega^- \\ w(\boldsymbol{x}) & \text{for } \boldsymbol{x} \in \Omega^+. \end{cases}$$

Applying a trace operator to the relation

$$D\phi(\boldsymbol{x}) + u^{\rm inc}(\boldsymbol{x}) = 0, \qquad \forall \boldsymbol{x} \in \Omega^-, \tag{77}$$

the physical unknown $\phi = -\gamma_0^+ w \in H^{1/2}(\Gamma)$ is solution to the following direct integral equations

- **EFIE :**
$$\mathcal{S}\phi = -\gamma_1^+ u^{\rm inc}, \quad \text{on } \Gamma. \tag{78}$$
- **MFIE :**
$$(-\frac{\mathcal{I}}{2} + \mathcal{D})\phi = -\gamma_0^+ u^{\rm inc}, \quad \text{on } \Gamma. \tag{79}$$
- **CFIE :**
$$\left\{(-\tfrac{\mathcal{I}}{2} + \mathcal{D}) + \eta\mathcal{S}\right\}\phi = -(\eta\gamma_1^+ u^{\rm inc}_{|\Gamma} + \gamma_0^+ u^{\rm inc}), \quad \text{on } \Gamma. \tag{80}$$

The existence and uniqueness results for the above integral equations are summarized in the next result.

Theorem 3. *The following properties hold*

1. *The operator $\mathcal{S}$ defines an isomorphism from $H^{1/2}(\Gamma)$ onto $H^{-1/2}(\Gamma)$ if and only if $k \notin K_N(\Omega^-)$. Under this condition, the EFIE* (78) *is uniquely solvable in $H^{1/2}(\Gamma)$.*

2. *The operator*

$$(-\frac{\mathcal{I}}{2}+\mathcal{D})$$

defines an isomorphism from $H^{1/2}(\Gamma)$ *onto* $H^{1/2}(\Gamma)$ *if and only if* $k \notin K_D(\Omega^-)$. *Under this condition, the MFIE* (79) *is uniquely solvable in* $H^{1/2}(\Gamma)$.

3. *The operator*

$$(-\frac{\mathcal{I}}{2}+\mathcal{D})+\eta\mathcal{S}$$

defines an isomorphism from $H^{1/2}(\Gamma)$ *onto* $H^{-1/2}(\Gamma)$ *for all* $k>0$ *provided* $\Im(\eta)\neq 0$. *Under this condition, the CFIE* (80) *is uniquely solvable in* $H^{1/2}(\Gamma)$ *for all frequency* $k>0$.

The reference CFIE in this chapter is

$$(1-\alpha)\frac{\iota}{k}(-\frac{\mathcal{I}}{2}+\mathcal{D})-\frac{\alpha}{k^2}\mathcal{S}=-((1-\alpha)\frac{\iota}{k}\gamma_0^+u^{\rm inc}-\frac{\alpha}{k^2}\gamma_1^+u^{\rm inc}),\quad \text{on } \Gamma. \tag{81}$$

3.4.4 The Neumann problem: indirect integral formulations

The Burton-Miller (or Brakhage-Werner) integral representation of the exterior field is expressed by

$$u^+(\boldsymbol{x})=(L+\eta D)\varphi(\boldsymbol{x}),\ \ \forall \boldsymbol{x}\in\Omega^+, \tag{82}$$

where η is a complex-valued coupling parameter to determine. Then, the field (82) solves the exterior boundary-value problem (42) if the surface density φ is solution to the following integral equation

$$\left\{(-\frac{\mathcal{I}}{2}+\mathcal{N})+\eta\mathcal{S}\right\}\varphi=-\gamma_1^+u^{\rm inc}, \tag{83}$$

called the Burton-Miller or Brakhage-Werner (BW) integral equation. We have the following existence and uniqueness result.

Theorem 4. *The operator*

$$(-\frac{\mathcal{I}}{2}+\mathcal{N})+\eta\mathcal{S}$$

defines an isomorphism from $H^{1/2}(\Gamma)$ *onto* $H^{-1/2}(\Gamma)$ *for all* $k>0$ *provided* $\Im(\eta)\neq 0$. *Under this condition,* (83) *is uniquely solvable in* $H^{1/2}(\Gamma)$ *for all frequency* $k>0$.

An almost optimal value of η has been numerically discussed in [2, 36, 38] as: $\eta=1/\iota k$.

4 Approximation of integral equations by boundary element methods

Integral equations are numerically by a boundary element method. We now describe how to develop this approximation for the EFIE for both the Dirichlet and Neumann problems. We also explain to extend the method to other standard integral equations. The numerical developments are made in the two-dimensional setting, the three-dimensional case being much harder.

4.1 The example of the single-layer representation (EFIE) for the Dirichlet problem

We describe now the numerical approximation methodology for solving the EFIE step by stepand next computing the relevant physical quantities.

Variational formulation and boundary element approximation.

In the two-dimensional case and for a Dirichlet boundary condition, let us recall that our scattering problem writes

$$\left\{ \begin{array}{l} \text{Find } p \in H^{-1/2}(\Gamma) \text{ such that} \\ \displaystyle\int_\Gamma G(\boldsymbol{x},\boldsymbol{y}) p(\boldsymbol{y}) d\Gamma(\boldsymbol{y}) = -u^{inc}, \qquad \text{in } H^{1/2}(\Gamma). \end{array} \right. \tag{84}$$

Like for PDEs where a finite element approach can be applied for a numerical solution after writing a weak formulation, the next step consists in taking the duality product of (84) for a test-function in $H^{-1/2}(\Gamma)$. Therefore, we are looking for the solution to the variational formulation

$$\left\{ \begin{array}{l} \text{Find } p \in H^{-1/2}(\Gamma) \text{ such that } \forall q \in H^{-1/2}(\Gamma) \\ < q, Gp >_{H^{-1/2}(\Gamma),H^{1/2}(\Gamma)} = - < q, u^{inc} >_{H^{-1/2}(\Gamma),H^{1/2}(\Gamma)} . \end{array} \right. \tag{85}$$

We assume now, for the sake of easiness, that Γ is sufficiently smooth so that $p \in L^2(\Gamma)$. Then, the duality product can be identified to the $L^2(\Gamma)$ usual hermitian product

$$(u,v)_{L^2(\Gamma)} = \int_\Gamma u \overline{v} d\Gamma. \tag{86}$$

As a consequence, our formulation can be written

$$\left\{ \begin{array}{l} \text{Find } p \in L^2(\Gamma) \text{ such that} \\ (\forall q \in L^2(\Gamma)), \displaystyle\int_\Gamma \int_\Gamma G(\boldsymbol{x},\boldsymbol{y}) p(\boldsymbol{y}) \overline{q}(\boldsymbol{x}) d\Gamma(\boldsymbol{y}) d\Gamma(\boldsymbol{x}) \\ \qquad\qquad\qquad\qquad = - \displaystyle\int_\Gamma u^{inc}(\boldsymbol{x}) \overline{q}(\boldsymbol{x}) d\Gamma(\boldsymbol{x}). \end{array} \right. \tag{87}$$

Let us now assume that we are working in the two-dimensional setting. The closed boundary is then a line in the $\mathbb{R}^2$ plane. We next introduce a polygonal curve Γ_h made of N_h segments $K_j = [\mathbf{a}_j^K; \mathbf{a}_{j+1}^K]$, for $j = 1, ..., N_h$. The length of K_j is denoted by

$$|K_j| := h_j = \text{meas}(K_j) = ||\mathbf{a}_j^K \mathbf{a}_{j+1}^K||, j = 1, ..., N_{h.} \tag{88}$$

Furthermore, the maximal step size is $h := \max_{j=1,...,N_h} h_j$. Then, we have

$$\Gamma_h = \cup_{j=1}^{N_h} K_j = \cup_{K \in \mathcal{T}_h} K, \tag{89}$$

and the surface triangulation is $\mathcal{T}_h = \{K_j\}_{j=1}^{N_h}$. In the three-dimensional setting, meshing is harder (see Fig. 12).

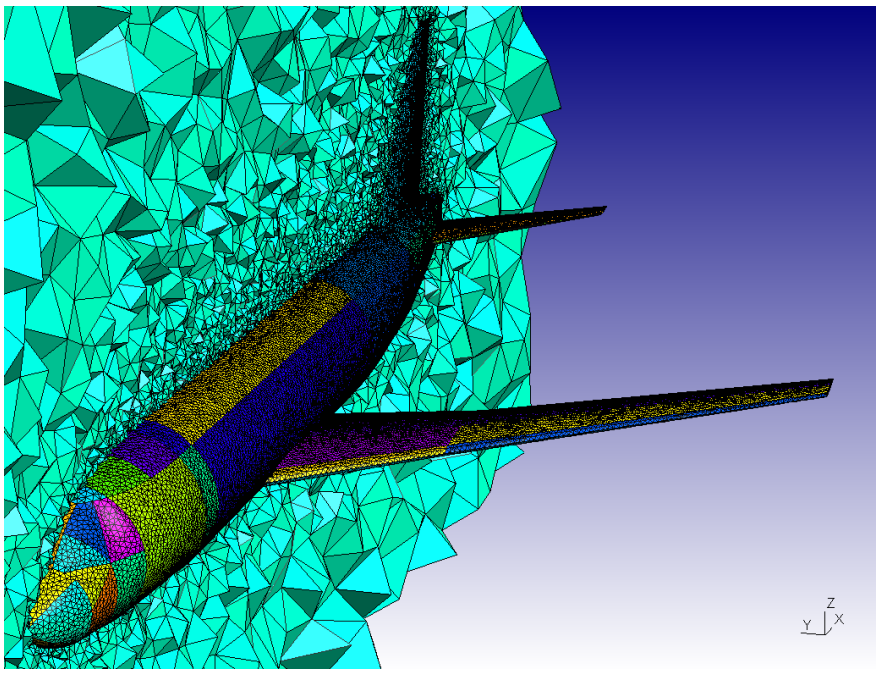

Figure 12: Designing meshes is harder in 3D (created with Gmsh).

Now that the surface is discretized, we must consider a finite dimensional space of approximation for p (and q). Since p is in $L^2(\Gamma)$ (or is even less regular), we can try to compute an approximation of p as a piecewise constant function per element K. Therefore, we introduce the finite element space

$$M_h := \left\{ q_h \in L^2(\Gamma_h) / q_K = q_{h|K} \in \mathbb{P}_0, \forall K \in \mathcal{T}_h \right\}, \tag{90}$$

where $\mathbb{P}_0$ designates the space of constant (polynomials). The weak continuous formulation (87) is then discretized as

$$\begin{cases} \text{Find } p_h \in M_h \text{ such that} \\ (\forall q_h \in M_h), \displaystyle\int_{\Gamma_h} \int_{\Gamma_h} G(\boldsymbol{x}_h, \boldsymbol{y}_h) p_h(\boldsymbol{y}_h) \overline{q_h}(\boldsymbol{x}_h) d\Gamma_h(\boldsymbol{y}_h) d\Gamma_h(\boldsymbol{x}_h) \\ \qquad\qquad = - \displaystyle\int_{\Gamma_h} u^{inc}(\boldsymbol{x}_h) \overline{q_h}(\boldsymbol{x}_h) d\Gamma_h(\boldsymbol{x}_h). \end{cases} \tag{91}$$

Let us now decompose p_h as

$$p_h = \sum_{segments} \text{constant per segment.} \tag{92}$$

The finite element method over the surface is generally called a boundary element method. Then, (91) leads to the solution of the linear system

$$\sum_{j=1}^{N_h} [[a]]_{i,j} p_j = b_i, 1 \leq i \leq N_h, \tag{93}$$

where

$$p_j := p_{h|K_j}, 1 \leq j \leq N_h, \tag{94}$$

and

$$b_i := -\int_{K_i} u^{inc}(\boldsymbol{x}_h) dK_i(\boldsymbol{x}_h), 1 \leq i \leq N_h. \tag{95}$$

More importantly, we have

$$1 \leq i, j \leq N_h, [[a]]_{i,j} := \int_{K_i} \int_{K_j} G(\boldsymbol{x}_h, \boldsymbol{y}_h) dK_j(\boldsymbol{y}_h) dK_i(\boldsymbol{x}_h). \tag{96}$$

Let us recall that the Green's function G is given by

$$G(\boldsymbol{x}, \boldsymbol{y}) = \frac{\iota}{4} H_0^{(1)}(k||\boldsymbol{x} - \boldsymbol{y}||), \boldsymbol{x} \neq \boldsymbol{y}, \tag{97}$$

and so is singular at the origin when $\boldsymbol{x} = \boldsymbol{y}$. Let us remind that the two points Gauss quadrature formula is given by

$$\int_{-1}^{+1} f(x) dx = \sum_{\ell=1}^{2} w_\ell f(x_\ell), \tag{98}$$

where the weights are $w_\ell = 1, 1$, for $\ell = 1, 2$, and the roots are $x_1 = -\sqrt{1/3}$ and $x_2 = \sqrt{1/3}$. It is easy to see that a change of variable provides the following integration formula

$$\int_a^b f(x) dx = \frac{(b-a)}{2} \int_{-1}^{+1} f(\frac{(b-a)}{2} x + \frac{a+b}{2}) dx \tag{99}$$

and then

$$\int_a^b f(x) dx \approx \frac{(b-a)}{2} \sum_{\ell=1}^{2} w_\ell f(\frac{(b-a)}{2} x_\ell + \frac{a+b}{2}). \tag{100}$$

Let us note

$$1 \leq i, j \leq N_h, [[a]]_{i,j} := \int_{K_i} g_{K_j}(\boldsymbol{x}_h) dK_i(\boldsymbol{x}_h), \tag{101}$$

with

$$1 \leq j \leq N_h, g_{K_j}(\boldsymbol{x}_h) := \int_{K_j} G(\boldsymbol{x}_h, \boldsymbol{y}_h) dK_j(\boldsymbol{y}_h) \\ = \int_{K_j} \frac{\iota}{4} H_0^{(1)}(k||\boldsymbol{x}_h - \boldsymbol{y}_h||) dK_j(\boldsymbol{y}_h). \tag{102}$$

For the numerical treatment, we separate the cases where K_i and K_j are different or not.

Situation 1: $K_i \neq K_j$ **(**$i \neq j$**):** In this situation, we can apply twice the Gauss quadrature formula to numerically integrate (101)-(102) by a double summation

$$1 \leq i, j \leq N_h, i \neq j, [[a]]_{i,j} = \sum_{\ell,m=1}^{2} w_\ell w_m G(\boldsymbol{x}_{h,\ell}^i, \boldsymbol{y}_{h,m}^j) \tag{103}$$

where $\boldsymbol{x}_{h,\ell}^i$ and $\boldsymbol{y}_{h,m}^j$ are the mapped Gauss points on the segments K_i and K_j, respectively.

Situation 2: $K_i = K_j$ **(**$i = j$**):** This situation is more delicate. Indeed, let us integrate once (101) by the Gauss quadrature (100). Then we obtain

$$i = 1, ..., N_h, [[a]]_{i,i} = \sum_{\ell=1}^{2} w_\ell g_{K_j}(\boldsymbol{x}_{h,\ell}^i), \tag{104}$$

with

$$g_{K_i}(\boldsymbol{x}_{h,\ell}^i) = \int_{K_i} G(\boldsymbol{x}_{h,\ell}^i, \boldsymbol{y}_h) dK_i(\boldsymbol{y}_h). \tag{105}$$

But the integral above cannot be directly approximated again by the Gauss quadrature since we have singularities at $\boldsymbol{x}_{h,\ell}^i = \boldsymbol{y}_{h,\ell}^i$. One way to overcome this problem is to use a semi-numerical quadrature approach based on the following splitting. Let us recall that the singularity of $H_0^{(1)}$ is logarithmic. More precisely, we have

$$G(\boldsymbol{x}, \boldsymbol{y}) = \frac{1}{2\pi} \ln \frac{1}{||\boldsymbol{x} - \boldsymbol{y}||} + \frac{\iota}{4} - \frac{1}{2} \ln(\frac{k}{2}) + \mathcal{O}(||\boldsymbol{x} - \boldsymbol{y}||^2 \ln(\frac{1}{||\boldsymbol{x} - \boldsymbol{y}||})) \tag{106}$$

for $||\boldsymbol{x} - \boldsymbol{y}|| \to 0$. This implies that we have the following decomposition

$$g_{K_j}(\boldsymbol{x}_h) = \int_{K_j} G(\boldsymbol{x}_h, \boldsymbol{y}_h) dK_j(\boldsymbol{y}_h) = \\ \int_{K_j} \frac{1}{2\pi} \ln \frac{1}{||\boldsymbol{x}_h - \boldsymbol{y}_h||} dK_j(\boldsymbol{y}_h) + \int_{K_j} \mathcal{K}(\boldsymbol{x}_h, \boldsymbol{y}_h) dK_j(\boldsymbol{y}_h) \tag{107}$$

The second integral which is related to the decomposition (106) involves a regular integrand $\mathcal{K}$ which therefore can be computed *via* (100). For the singular part, we can use the Hoop formula that provides an explicit analytical formula for the logarithmic singularity. We have

$$\int_{K_j} -\frac{1}{2\pi} \ln ||\boldsymbol{x}_h - \boldsymbol{y}_h|| dK_j(\boldsymbol{x}_h) \\ = -\frac{1}{2\pi} (\boldsymbol{R}_{j+1}^K \cdot \boldsymbol{\tau}_{K_j} \ln ||\boldsymbol{R}_{j+1}^K|| - \boldsymbol{R}_j^K \cdot \boldsymbol{\tau}_{K_j} \ln ||\boldsymbol{R}_j^K||) \\ -|K_j| + d_{K_j}(\boldsymbol{x}_h)\Omega. \tag{108}$$

In the above formula, we use the following notations

$$\left\{\begin{array}{l} \boldsymbol{\tau}_{K_j} = \text{tangential unit vector} = \dfrac{\mathbf{a}_j^K \mathbf{a}_{j+1}^K}{|K_j|}, \\ \boldsymbol{R}_j^K = \boldsymbol{x}_h \mathbf{a}_j^K, \boldsymbol{R}_{j+1}^K = \boldsymbol{x}_h \mathbf{a}_{j+1}^K, \\ d_{K_j}(\boldsymbol{x}_h) = \text{dist}_{K_j}^{\perp}(\boldsymbol{x}_h) : \text{distance from } \boldsymbol{x}_h \text{ to } K_j, \\ \Omega = \text{solid angle under which } \boldsymbol{x}_h \text{ sees } K_j, \, 0 \leq \Omega \leq \pi. \end{array}\right. \tag{109}$$

Since $K_j = K_i$, then $\Omega = 0$ and $d_{K_j}(\boldsymbol{x}_h) = 0$, which simplifies (108). An illustration of the notations is given on the figure below.

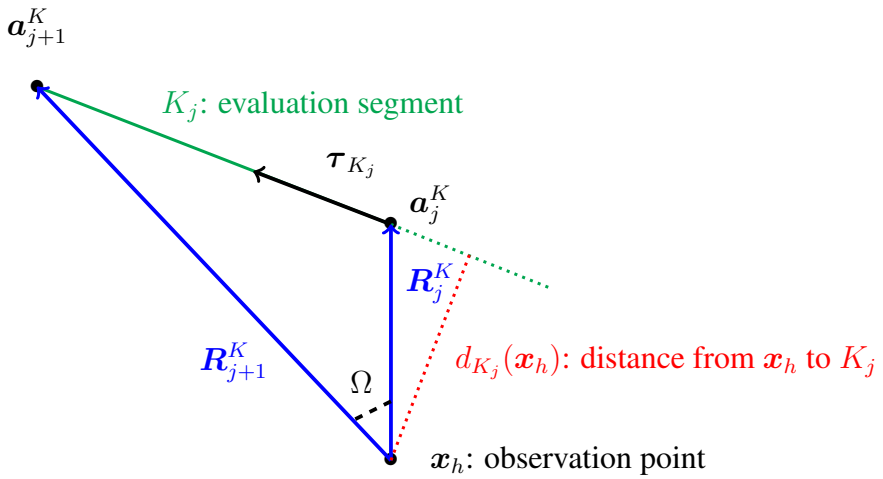

Let us now consider that we have been able to compute the matrix coefficients $[[a]]_{i,j}$, for $1 \leq i, j \leq N_h$. We have to approximate the right hand side by computing

$$b_i := -\int_{K_i} u^{inc}(\boldsymbol{x}_h) dK_i(\boldsymbol{x}_h), 1 \leq i \leq N_h \tag{110}$$

which can be directly done by the Gauss quadrature formula.

Linear system solution.

Finally, (93) leads to solving a linear system

$$\mathbb{A}\mathbf{p}_h = \mathbf{b}_h \tag{111}$$

with

$$\left\{\begin{array}{l} \mathbb{A}_{ij} = [[a]]_{ij} \in \mathbb{C}, 1 \leq i, j \leq N_h \\ \mathbf{p}_h \in \mathbb{C}^{N_h}, \mathbf{b}_h \in \mathbb{C}^{N_h}. \end{array}\right. \tag{112}$$

System (111) is full, complex-valued, symmetrical but non definite positive. For relatively moderate values of N_h, the linear system can be solved by a Gauss elimination solver. However, for larger values of N_h, Krylov solvers are preferred (most particularly for three-dimensional problems) in conjunction with a fast matrix-vector product evaluation (integral evaluations in fact) based on Multilevel Fast Multipole Methods (MFMM) or closely related techniques. We refer to the specialized literature for further details.

Computing relevant physical quantities.

Once p_h has been computed, the exterior wavefield u^+ can be obtained *via* relation (68), that is

$$u^+(\boldsymbol{x}) = \int_\Gamma G(\boldsymbol{x},\boldsymbol{y})p(\boldsymbol{y})d\Gamma(\boldsymbol{y}) \tag{113}$$

which is discretized by

$$\begin{aligned} u_h^+(\boldsymbol{x}_h) &= \int_{\Gamma_h} G(\boldsymbol{x}_h,\boldsymbol{y}_h)p_h(\boldsymbol{y}_h)d\Gamma_h(\boldsymbol{y}_h) = \sum_{j=1}^{N_h}\int_{K_j} G(\boldsymbol{x}_h,\boldsymbol{y}_h)p_j dK_j(\boldsymbol{y}_h) \\ &\approx \sum_{j=1}^{N_h}(\sum_{\ell=1}^{2} w_\ell G(\boldsymbol{x}_h,\boldsymbol{y}_{h,\ell}^j))p_j \end{aligned} \tag{114}$$

Another interesting quantity is the normal derivative trace of u^+ which is trivially obtained by the relation

$$p = [\partial_{\boldsymbol{n}} u]_\Gamma = -\partial_{\boldsymbol{n}} w = -\partial_{\boldsymbol{n}} u^+ - \partial_{\boldsymbol{n}} u^{inc}$$

and so

$$\partial_{\boldsymbol{n}} u^+ = -p - \partial_{\boldsymbol{n}} u^{inc}, \text{on } \Gamma.$$

Finally, a last quantity of interest is the so-called Radar (or Sonar, echowidth) Cross Section. This quantity describes the gain of the incident plane wave created by the presence of the scatterer and is defined, for the two-dimensional case, by

$$\left\{ \begin{array}{l} \lim\limits_{r\to+\infty} 2\pi r \dfrac{|u^+(\boldsymbol{x})|^2}{|u^{inc}(\boldsymbol{x})|^2} = 2\pi|a_0(\theta)|^2 \\ \text{RCS}(\theta) := 10\log_{10}(2\pi|a_0(\theta)|^2)\text{(dB) (decibels).} \end{array} \right. \tag{115}$$

It can be proved that, in the far-field, the scattered field behaves like

$$u^+(\boldsymbol{x}) \approx_{r\to+\infty} \frac{e^{\iota kr}}{\sqrt{r}} a_0(\theta) + o(\frac{1}{\sqrt{r}}) \tag{116}$$

in the polar coordinates system. The scattering amplitude a_0 is therefore the quantity to determine. However, in the far-field, we have

$$a_0(\theta) = e^{\iota\pi/4}\frac{1}{\sqrt{8\pi k}}\int_\Gamma p(\boldsymbol{y})e^{-\iota k\boldsymbol{\theta}\cdot\boldsymbol{y}}d\Gamma(\boldsymbol{y}) \tag{117}$$

with $\boldsymbol{\theta} = (\cos\theta, \sin\theta)$. This means that knowing an evaluation of p allows through (117) to obtain an numerical estimation of a_0.

4.2 The example of the Neumann problem by using the EFIE

As for the Dirichlet problem, we follow the usual approach for numerically solving our problem based on weak formulation with boundary element methods.

Variational formulation and boundary element approximation.

Let us consider the Neumann problem solved by the EFIE (78)

$$\left\{ \begin{array}{l} \text{Find } \phi \in H^{1/2}(\Gamma) \text{ such that} \\ \mathcal{S}\phi = -\partial_{\boldsymbol{n}} u^{\text{inc}}, \text{ in } H^{-1/2}(\Gamma). \end{array} \right. \tag{118}$$

Let us assume that we have a test-function $\phi' \in H^{1/2}(\Gamma)$. Then, we have to solve the following weak formulation

$$\left\{ \begin{array}{l} \text{Find } \phi \in H^{1/2}(\Gamma) \text{ such that } \forall \phi' \in H^{1/2}(\Gamma) \\ < \mathcal{S}\phi, \phi' >_{H^{-1/2}(\Gamma), H^{1/2}(\Gamma)} = - < \partial_{\boldsymbol{n}} u^{\text{inc}}, \phi' >_{H^{-1/2}(\Gamma), H^{1/2}(\Gamma)} . \end{array} \right. \tag{119}$$

We make the assumption, for regularity reasons, that $\partial_{\boldsymbol{n}} u^{\text{inc}} \in H^{1/2}(\Gamma)$. Again, by identification of the dual product and the hermitian product and since $H^{1/2}(\Gamma)$ is a subset of $L^2(\Gamma)$, our problem is now

$$\left\{ \begin{array}{l} \text{Find } \phi \in H^{1/2}(\Gamma) \text{ such that } \forall \phi' \in H^{1/2}(\Gamma) \\ \displaystyle\int_\Gamma \int_\Gamma \frac{\partial^2 G}{\partial \boldsymbol{n}(\boldsymbol{x}) \partial \boldsymbol{n}(\boldsymbol{y})}(\boldsymbol{x}, \boldsymbol{y}) \phi(\boldsymbol{y}) \phi'(\boldsymbol{x}) d\Gamma(\boldsymbol{y}) d\Gamma(\boldsymbol{x}) \\ \qquad\qquad = - \displaystyle\int_\Gamma \partial_{\boldsymbol{n}} u^{\text{inc}}(\boldsymbol{x}) \phi'(\boldsymbol{x}) d\Gamma(\boldsymbol{x}) \end{array} \right. \tag{120}$$

We have seen that $\mathcal{S}$ is a hypersingular integral operator. By using a new weak form of this operator based on an integration by parts, we show that we can have a weaker singularity which is easier to compute. To this end, let us consider the following result.

Proposition 5. *Let ϕ be a density defined over the surface Γ. The double-layer potential is defined by*

$$D\phi(\boldsymbol{x}) := \int_\Gamma \partial_{\boldsymbol{n}(\boldsymbol{y})} G(\boldsymbol{x}, \boldsymbol{y}) \phi(\boldsymbol{y}) d\Gamma(\boldsymbol{y}), \quad \boldsymbol{x} \notin \Gamma.$$

Then, the trace of the gradient of D satisfies the relation

$$\begin{array}{rl} \nabla_{\boldsymbol{x}} D\varphi(\boldsymbol{x}) = \pm \dfrac{1}{2} \nabla_\Gamma \phi(\boldsymbol{x}) + k^2 \displaystyle\int_\Gamma G(\boldsymbol{x}, \boldsymbol{y}) \phi(\boldsymbol{y}) \boldsymbol{n}(\boldsymbol{y}) d\Gamma(\boldsymbol{y}) \\ \qquad\qquad - \displaystyle\int_\Gamma \nabla_{\boldsymbol{x}} G(\boldsymbol{x}, \boldsymbol{y}) \times [\nabla_\Gamma \phi(\boldsymbol{y}) \times \boldsymbol{n}(\boldsymbol{y})] d\Gamma(\boldsymbol{y}) \end{array} \tag{121}$$

for $\boldsymbol{x} \in \Gamma$.

Hereabove, ∇_Γ designates the surface gradient (of a scalar surface field). In the two-dimensional case, we can prove that: $\nabla_\Gamma = \partial_s$, where s is the curvilinear abscissa along Γ. The operator $\nabla_{\boldsymbol{x}}$ is the gradient with respect to the $\boldsymbol{x}$ variable and $\boldsymbol{a} \times \boldsymbol{b}$ is the usual vector product of two complex valued vector fields $\boldsymbol{a}$ and $\boldsymbol{b}$ in $\mathbb{R}^d$.

We use now Proposition 5 to rewrite the formulation (120). Let us consider $\nabla_{\boldsymbol{x}} D(\boldsymbol{x}) \cdot \boldsymbol{n}(\boldsymbol{x})$ on Γ

$$\begin{aligned} \nabla_{\boldsymbol{x}} D(\boldsymbol{x}) \cdot \boldsymbol{n}(\boldsymbol{x}) = k^2 \int_\Gamma G(\boldsymbol{x},\boldsymbol{y}) \phi(\boldsymbol{y}) \boldsymbol{n}(\boldsymbol{y}) \cdot \boldsymbol{n}(\boldsymbol{x}) d\Gamma(\boldsymbol{y}) \\ - \int_\Gamma \nabla_{\boldsymbol{x}} G(\boldsymbol{x},\boldsymbol{y}) \times [\nabla_\Gamma \phi(\boldsymbol{y}) \times \boldsymbol{n}(\boldsymbol{y})] \cdot \boldsymbol{n}(\boldsymbol{x}) d\Gamma(\boldsymbol{y}) \end{aligned} \tag{122}$$

for $\boldsymbol{x} \in \Gamma$. Indeed, since $\nabla_\Gamma \phi$ is in the tangent plane to Γ at the evaluation point $\boldsymbol{x}$, we have

$$\nabla_\Gamma \phi(\boldsymbol{x}) \cdot \boldsymbol{n}(\boldsymbol{x}) = 0, \forall \boldsymbol{x} \in \Gamma.$$

We also have the relation

$$\begin{aligned} \int_\Gamma \nabla_{\boldsymbol{x}} G(\boldsymbol{x},\boldsymbol{y}) \times [\nabla_\Gamma \phi(\boldsymbol{y}) \times \boldsymbol{n}(\boldsymbol{y})] \cdot \boldsymbol{n}(\boldsymbol{x}) d\Gamma(\boldsymbol{y}) \\ = - \int_\Gamma \nabla_{\boldsymbol{x}} G(\boldsymbol{x},\boldsymbol{y}) \times \boldsymbol{n}(\boldsymbol{x}) \cdot [\nabla_\Gamma \phi(\boldsymbol{y}) \times \boldsymbol{n}(\boldsymbol{y})] d\Gamma(\boldsymbol{y}) \end{aligned} \tag{123}$$

since we have the following vector algebra relation: $(\boldsymbol{a} \times \boldsymbol{b}) \cdot \boldsymbol{c} = -(\boldsymbol{a} \times \boldsymbol{c}) \cdot \boldsymbol{b}$, for vectors $\boldsymbol{a}, \boldsymbol{b}$ and $\boldsymbol{c}$ in $\mathbb{C}^d$. Combining this equation with (120) and considering the integration product with a test-function ϕ' in $H^{1/2}(\Gamma)$ gives

$$\begin{aligned} \int_\Gamma \int_\Gamma \nabla_{\boldsymbol{x}} G(\boldsymbol{x},\boldsymbol{y}) \times \boldsymbol{n}(\boldsymbol{x}) \cdot [\nabla_\Gamma \phi(\boldsymbol{y}) \times \boldsymbol{n}(\boldsymbol{y})] \phi'(\boldsymbol{x}) d\Gamma(\boldsymbol{y}) d\Gamma(\boldsymbol{x}) \\ + k^2 \int_\Gamma \int_\Gamma G(\boldsymbol{x},\boldsymbol{y}) \phi(\boldsymbol{y}) \phi'(\boldsymbol{x}) \boldsymbol{n}(\boldsymbol{y}) \cdot \boldsymbol{n}(\boldsymbol{x}) d\Gamma(\boldsymbol{y}) d\Gamma(\boldsymbol{x}) \\ = - \int_\Gamma \partial_{\boldsymbol{n}} u^{\mathrm{inc}}(\boldsymbol{x}) \phi'(\boldsymbol{x}) d\Gamma(\boldsymbol{x}). \end{aligned} \tag{124}$$

To simplify, let us assume now that we are in the two-dimensional case. Then, we have: $\boldsymbol{a} \times \boldsymbol{b} := a_1 b_2 - b_1 a_2$ and

$$\begin{aligned} \nabla_\Gamma \phi(\boldsymbol{y}) \times \boldsymbol{n}(\boldsymbol{y}) = \partial_{x_1} \phi(\boldsymbol{y}) n_2(\boldsymbol{y}) - \partial_{x_2} \phi(\boldsymbol{y}) n_1(\boldsymbol{y}) \\ = -\nabla_\Gamma \phi(\boldsymbol{y}) \cdot \boldsymbol{\tau}(\boldsymbol{y}) = -\partial_{s(\boldsymbol{y})} \phi(\boldsymbol{y}). \end{aligned} \tag{125}$$

Hence, Eq. (123) writes

$$\begin{aligned} \int_\Gamma \int_\Gamma \partial_{s(\boldsymbol{x})} G(\boldsymbol{x},\boldsymbol{y}) (\partial_{s(\boldsymbol{y})} \phi(\boldsymbol{y})) \phi'(\boldsymbol{x}) d\Gamma(\boldsymbol{y}) d\Gamma(\boldsymbol{x}) \\ = - \int_\Gamma \int_\Gamma G(\boldsymbol{x},\boldsymbol{y}) \partial_{s(\boldsymbol{y})} \phi(\boldsymbol{y}) \partial_{s(\boldsymbol{x})} \phi'(\boldsymbol{x}) d\Gamma(\boldsymbol{y}) d\Gamma(\boldsymbol{x}) \end{aligned} \tag{126}$$

and Eq. (124) gives

$$\begin{aligned} \int_\Gamma \int_\Gamma G(\boldsymbol{x},\boldsymbol{y}) (\partial_{s(\boldsymbol{y})} \phi(\boldsymbol{y}) \partial_{s(\boldsymbol{x})} \phi'(\boldsymbol{x}) - k^2 \phi(\boldsymbol{y}) \phi'(\boldsymbol{x}) \boldsymbol{n}(\boldsymbol{y}) \cdot \boldsymbol{n}(\boldsymbol{x})) d\Gamma(\boldsymbol{y}) d\Gamma(\boldsymbol{x}) \\ = \int_\Gamma \partial_{\boldsymbol{n}} u^{\mathrm{inc}}(\boldsymbol{x}) \phi'(\boldsymbol{x}) d\Gamma(\boldsymbol{x}) \end{aligned} \tag{127}$$

for any test-function ϕ' in $H^{1/2}(\Gamma)$. In the three-dimensional case, one would obtain (after a suitable integration by part) the following formulation

$$\left\{\begin{array}{l} \text{Find } \phi \in H^{1/2}(\Gamma) \text{ such that } \forall \phi' \in H^{1/2}(\Gamma) \\ \displaystyle\int_\Gamma \int_\Gamma G(\boldsymbol{x},\boldsymbol{y}) \left\{ [\nabla_\Gamma \phi(\boldsymbol{y}) \times \boldsymbol{n}(\boldsymbol{y})] \cdot [\nabla_\Gamma \phi'(\boldsymbol{x}) \times \boldsymbol{n}(\boldsymbol{x})] \right. \\ \qquad\qquad \left. -k^2 (\phi \boldsymbol{n})(\boldsymbol{y}) \cdot (\phi' \boldsymbol{n})(\boldsymbol{x}) \right\} d\Gamma(\boldsymbol{y}) d\Gamma(\boldsymbol{x}) \\ \qquad\qquad = \displaystyle\int_\Gamma \partial_{\boldsymbol{n}} u^{\mathrm{inc}}(\boldsymbol{x}) \phi'(\boldsymbol{x}) d\Gamma(\boldsymbol{x}) \end{array}\right. \tag{128}$$

Concerning the numerical approximation, the surface Γ is approximated like before by a collection of segments: $\Gamma_h = \cup_{j=1}^{N_h} K_j$. The main difference is that, this time, derivatives $\partial_s \phi$ arise in the formulations. Therefore, a boundary element method based on piecewise linear elements must be used. For that reason, we introduce the following finite element space

$$V_h := \left\{ \phi'_h \in \mathcal{C}^0(\Gamma_h); \phi'_K := \phi'_{h|K} \in \mathbb{P}_1, \forall K \in \mathcal{T}_h \right\}. \tag{129}$$

The degrees of freedom are the values of the surface field ϕ_h at the nodes $\left\{ \mathbf{a}_j^K \right\}_{j=1}^{N_h}$ of the mesh Γ_h.

Let us introduce the usual way of defining a mesh with its connectivity tables: $(\mathtt{n}, \mathtt{T}, \mathtt{e})$. We define

- $\mathtt{n}$: the size of this two-dimensional array is the number of nodes of the triangulation times the dimension d plus 1. For $\ell = 1, ..., \sharp$nodes, and $j = 1$, we have the global label of the node: $\mathtt{n}(\ell, 1) = \ell$, and $(\mathtt{n}(\ell, j))_{j=2,...,d+1}$ represents the node $\mathbf{a}_{h,\ell}^K = (a_{h,\ell,1}^K, ..., a_{h,\ell,d}^K)$.
- $\mathtt{T}$ is a two-dimensional array which gives the triangle list with their vertices: $\mathtt{T}(l, :)$ is the ℓ-th triangle of the triangulation, $1 \leq \ell \leq N_h$, and $\mathtt{T}(\ell, 1)$ its global number, $\mathtt{T}(\ell, 2 : d+2)$ the global label of its $(d+1)$ vertices.
- $\mathtt{e}$: is an array that provides some informations related to the edges of the triangulation but that we do not use here.

Let us consider two segments K and L of $\mathcal{T}_h$ and let us compute their contribution during the assembly process. We have to calculate the contribution

$$\begin{array}{l} \displaystyle\int_K \int_L G(\boldsymbol{x},\boldsymbol{y}) (\partial_{s(\boldsymbol{y})} \phi(\boldsymbol{y}) \partial_{s(\boldsymbol{x})} \phi'(\boldsymbol{x}) \\ \qquad\qquad - k^2 \phi(\boldsymbol{y}) \phi'(\boldsymbol{x}) \boldsymbol{n}(\boldsymbol{y}) \cdot \boldsymbol{n}(\boldsymbol{x})) dL(\boldsymbol{y}) dK(\boldsymbol{x}) \end{array} \tag{130}$$

in the global linear system for two linear test-functions $\phi_{|K}$ and $\phi'_{|L}$, respectively. They can be written

$$\left\{\begin{array}{l} \phi_{|K} = (1 - \dfrac{s_K}{|K|}) \phi(\mathbf{a}_K^1) + \dfrac{s_K}{|K|} \phi(\mathbf{a}_K^2), 1 \leq s_K \leq |K|, \\ \phi'_{|L} = (1 - \dfrac{s_L}{|L|}) \phi'(\mathbf{a}_L^1) + \dfrac{s_L}{|L|} \phi'(\mathbf{a}_L^2), 1 \leq s_L \leq |L|. \end{array}\right. \tag{131}$$

Therefore, we have

$$\phi_{|K}(\mathbf{a}_K^j) = \phi(\mathbf{a}_K^j), j = 1, 2,$$

and

$$\begin{cases} \partial_s \phi_{|K} = \dfrac{1}{|K|}(\phi(\mathbf{a}_K^2) - \phi(\mathbf{a}_K^1)), \\ \partial_s \phi'_{|L} = \dfrac{1}{|L|}(\phi'(\mathbf{a}_L^2) - \phi'(\mathbf{a}_L^1)). \end{cases} \tag{132}$$

Furthermore, we approximate $\phi_{|L}$ and $\phi'_{|K}$ by their respective averages

$$\begin{cases} \phi_{|K} = \dfrac{\phi(\mathbf{a}_K^1) + \phi(\mathbf{a}_K^2)}{2} \\ \phi'_{|L} = \dfrac{\phi'(\mathbf{a}_L^1) + \phi'(\mathbf{a}_L^2)}{2} \end{cases} \tag{133}$$

Moreover, $\boldsymbol{n}(\boldsymbol{x})_{|K} = \boldsymbol{n}_K$ and $\boldsymbol{n}(\boldsymbol{y})_{|L} = \boldsymbol{n}_L$ are constant on each element. Finally, (130) is approximated by

$$[\phi'(\mathbf{a}_L^1); \phi'(\mathbf{a}_L^2)]\mathbb{B}_{KL}[\phi(\mathbf{a}_K^1); \phi(\mathbf{a}_K^2)]^T \tag{134}$$

where

$$\mathbb{B}_{KL} = \mathbb{A}_{KL}\left\{ \frac{1}{|K||L|}\begin{pmatrix} 1 & -1 \\ -1 & 1 \end{pmatrix} - \frac{k^2}{4}\boldsymbol{n}_K \cdot \boldsymbol{n}_L \begin{pmatrix} 1 & 1 \\ 1 & 1 \end{pmatrix} \right\} \tag{135}$$

Here, $\mathbb{A}_{KL}$ is given by

$$\mathbb{A}_{KL} := \int_K \int_L G(\boldsymbol{x}_h, \boldsymbol{y}_h) dL(\boldsymbol{y}_h) dK(\boldsymbol{x}_h) \tag{136}$$

and can be computed like for the Dirichlet problem by a semi analytical quadrature formula.

Let us consider now the right hand side. We use the following approximation

$$\begin{aligned} \int_L \partial_{\boldsymbol{n}} u^{\mathrm{inc}}(\boldsymbol{x})_{|L} \phi'(\boldsymbol{x}) dL(\boldsymbol{x}) &\approx [\phi'(\mathbf{a}_L^1); \phi'(\mathbf{a}_L^2)] \frac{|L|}{2} \partial_{\boldsymbol{n}_L} u^{\mathrm{inc}}(\boldsymbol{x})_{|L} \\ &= [\phi'(\mathbf{a}_L^1); \phi'(\mathbf{a}_L^2)] \cdot [\frac{|L|}{2} \partial_{\boldsymbol{n}_L} u^{\mathrm{inc}}(\boldsymbol{x})_{|L}; \frac{|L|}{2} \partial_{\boldsymbol{n}_L} u^{\mathrm{inc}}(\boldsymbol{x})_{|L}] \end{aligned} \tag{137}$$

Linear system solution.

Finally, the assembly process which consists in summing all the elementary integrals over the triangulation provides the global linear system to solve. This system is complex-valued of size $N_h \times N_h$, symmetrical and non definite positive. It writes down: $\mathbb{A}\boldsymbol{\phi} = \mathbf{b}$ and is created by the assembly procedure below for the two-dimensional Neumann problem

Assembly procedure

for $m = 1, ..., N_h$ **do**
  $[m_1, m_2] = \mathtt{T}(m, 2:3)$
  $\mathbf{a}_K^1 = \mathtt{n}(m_1, 2:3)$
  $\mathbf{a}_K^2 = \mathtt{n}(m_2, 2:3)$
  for $\ell = 1, ..., N_h$ **do**
    $[\ell_1, \ell_2] = \mathtt{T}(\ell, 2:3)$
    $\mathbf{a}_L^1 = \mathtt{n}(\ell_1, 2:3)$
    $\mathbf{a}_L^2 = \mathtt{n}(\ell_2, 2:3)$
    $\mathbb{A}_{KL} := \mathtt{integrate}(K, L, G)$
    $\mathtt{compute}\ \mathbb{B}_{KL}\ (2 \times 2\ \mathtt{elementary\ matrix})$
    for $p = 1, 2$ **do**
      for $q = 1, 2$ **do**
        $\mathbb{A}(\mathtt{T}(\ell, p+1), \mathtt{T}(m, q+1))$
          $= \mathbb{A}(\mathtt{T}(\ell, p+1), \mathtt{T}(m, q+1)) + \mathbb{A}_{KL} * \mathbb{B}_{KL}(p, q)$
      end for
    end for
    $\mathbf{b}(\mathtt{T}(\ell, p+1)) = \mathbf{b}(\mathtt{T}(\ell, p+1)) + \dfrac{|L|}{2} \partial_{\boldsymbol{n}} u^{\mathrm{inc}}(\boldsymbol{x})_{|L}$
  end for
end for

Computing relevant physical quantities.

Finally, the different physical quantities can be computed by using the integral equation representation based on the double-layer potential

$$u^+(\boldsymbol{x}) = D\phi(\boldsymbol{x}), \quad \boldsymbol{x} \in \Omega^+. \tag{138}$$

The surface trace of the field is obtained through the density and the far field pattern by the relation

$$a_0(\theta) = e^{-\iota\pi/4} \frac{k}{\sqrt{8\pi}} \int_\Gamma \phi(\boldsymbol{y}) e^{-\iota k \boldsymbol{\theta}\cdot\boldsymbol{y}} \boldsymbol{\theta} \cdot \boldsymbol{n}(\boldsymbol{y}) d\Gamma(\boldsymbol{y}) \tag{139}$$

4.3 Extension to other kinds of integral equations

Essentially, for the other formulations, that is the CFIE and Brakhage-Werner equations, we have to be able to approximate the trace of the double-layer potential

$$\mathcal{D}\phi(\boldsymbol{x}) := \int_\Gamma \partial_{\boldsymbol{n}(\boldsymbol{y})} G(\boldsymbol{x}, \boldsymbol{y}) \phi(\boldsymbol{y}) d\Gamma(\boldsymbol{y}) \tag{140}$$

for $\boldsymbol{x} \in \Gamma$ since it can be proven that $\mathcal{D} = \mathcal{N}^T$. By using (106) we have for two segments

$$\begin{aligned}\int_{K_j} \partial_{\boldsymbol{n}_{K_j}(\boldsymbol{y}_h)} G(\boldsymbol{x}_h, \boldsymbol{y}_h) dK_j(\boldsymbol{y}_h) = \\ - \int_{K_j} \frac{1}{2\pi} \partial_{\boldsymbol{n}_{K_j}(\boldsymbol{y}_h)} \ln \frac{1}{||\boldsymbol{x}_h - \boldsymbol{y}_h||} dK_j(\boldsymbol{y}_h) \\ + \int_{K_j} \mathcal{L}(\boldsymbol{x}_h, \boldsymbol{y}_h) \frac{\boldsymbol{y}_h - \boldsymbol{x}_h}{||\boldsymbol{y}_h - \boldsymbol{x}_h||} \cdot \boldsymbol{n}_{K_j}(\boldsymbol{y}_h) dK_j(\boldsymbol{y}_h)\end{aligned} \tag{141}$$

where $\mathcal{L}$ is a smooth function to integrate. Concerning the integration of the new singularity, we have that

$$- \int_{K_j} \frac{1}{2\pi} \partial_{\boldsymbol{n}_{K_j}(\boldsymbol{y}_h)} \ln \frac{1}{||\boldsymbol{x}_h - \boldsymbol{y}_h||} dK_j(\boldsymbol{y}_h) = -\frac{\Omega}{2\pi},$$

where Ω is the solid angle previously defined.

5 Examples of numerical simulations based on integral equations

We provide a few numerical examples for two- and three-dimensional computations. The two-dimensional simulations have been obtained with a Matlab code based on the methods presented in the paper. The three-dimensional simulations are provided by Marion Darbas (Amiens University, France), Eric Darrigrand and Yvon Lafranche (Rennes University, France) by using the freely available solver `Melina++`[19]. Another open source boundary element solver solver is developed by Stephen Kirkup[20]. Meshing generation in two-dimensions is home made but the three-dimensional meshes use `Gmsh`[21] which is also a freely distributed powerful mesh generator created by Christophe Geuzaine (Liège University, Belgium) and Jean-François Remacle (Louvain University, Belgium).

5.1 Two-dimensional scattering

On the first picture of Fig. 13, we consider an exterior Dirichlet problem where the obstacle is the square cylinder centered at the origin and with a side length equals to 2. The incident wave is characterized by a frequency $k = 14$ and a null-incidence. On the second picture of Fig. 13, we consider an incident field whose wave number is $k = 20$ and with a 45 deg. angle of attack for the Neumann problem. The obstacle is a conesphere with a tip in the (Ox_1)-direction. The integral equation solution is labelled by BIEM and obtained by the EFIE formulation (the other curve corresponds to an

[19] Melina

[20] S. Kirkup's boundary element solver

[21] Gmsh

asymptotic numerical solution called OSRC that we do not develop here). On these two figures, we can see where most of the scattering arises, according to the frequency and shape of the scatterer (you can do draw the obstacle and try to understand the main scattering radiation).

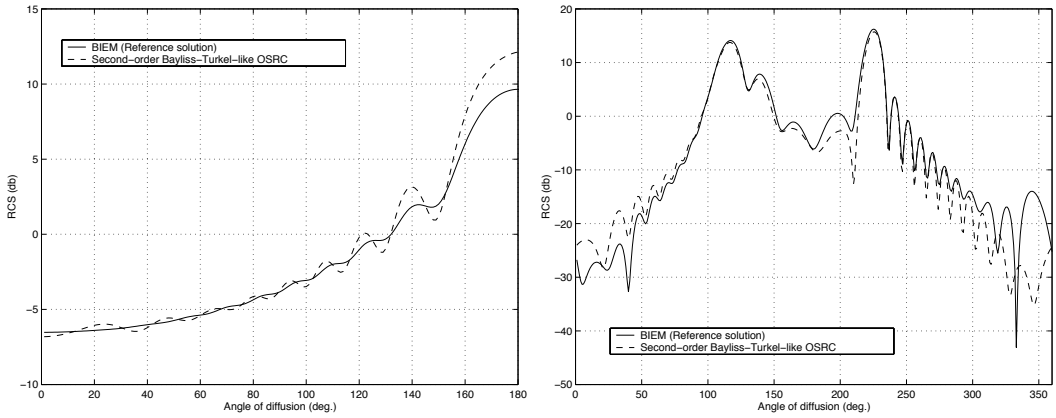

Figure 13: Computation of the bistatic RCS: Case 1: a plane wave of characteristics $k = 14$ and $\theta^{\text{inc}} = 0$ deg. illuminates the unit square cylinder for a Dirichlet boundary condition, Case 2: a plane wave of characteristics $k = 20$ and $\theta^{\text{inc}} = 45$ deg. illuminates a conesphere for a Neumann boundary condition.

5.2 Three-dimensional scattering

We did not develop the numerical method for the three-dimensional case. In some way, the method is close to the two-dimensional case but at the same time much more technical concerning the way of creating of surface mesh, integrating the singularities and doing the assembly process. Furthermore, the full complex valued linear system to solve is pretty big and requires the help of adapted numerical methods based on Multilevel Fast Multipole Methods (FMM) and Krylov solvers. This is the case of the following computations which present RCS calculations that use a generalization of the CFIE based on asymptotic methods (the η parameter in the formulations is replaced by a suitable operator) solved by the GMRES and FMM. The method is therefore called CFIE+OSRC+FMM. If the CFIE is solved by a Gauss elimination method, then it is called CFIE. CFIE+ FMM refers to the Krylov solution of the CFIE with the standard parameter η given previously. All our examples concern the Neumann problem solved by a linear boundary element method.

In the first examples presented on Figures 14 we report the RCS in the (x_1, x_2)-plane for different increasing wave numbers and adapted triangular surface meshes.

The number of triangles is given at each time and provides informations on the size of the linear system to solve. Furthermore, the Fourier series expansion, usually called Mie series solution, is also reported for comparison purpose. We can see that high accuracy is obtained, small oscillations appear when the high frequency regime is

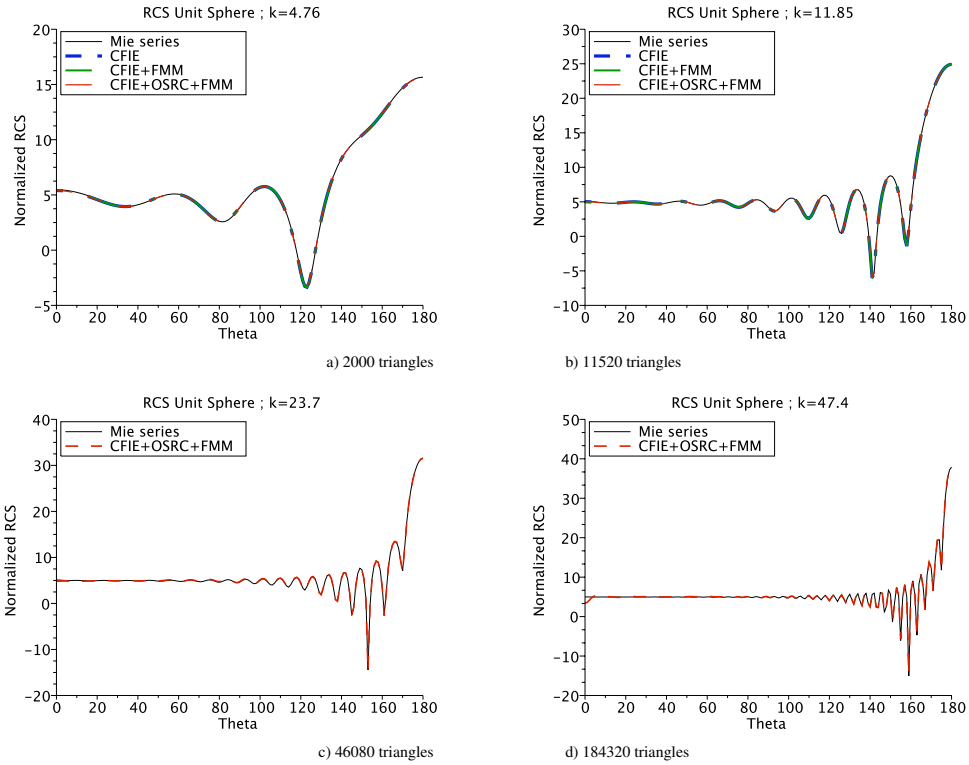

Figure 14: Scattering by a sphere (null incidence)

reached and small amplitude field oscillations can be observed in the shadow region. Let us note that for the two last pictures, only the CFIE+OSRC+FMM allows to obtain the results, the two others being too expensive or converge too slowly.

To have an idea of the CPU time that are necessary even for these performant codes we report below the results. As you can see large computational times are generally required even for the sphere. This clearly is harder for large wave numbers since many degrees of freedom are necessary.

Computation costs

k	Total CPU time CFIE	Total CPU time CFIE + SLFMM	Total CPU time CFIE + SLFMM + OSRC
4.76	7 min 42”	13 min	2 min 42”
11.85	9 h 43 min	4 h 33 min	32 min 40”
23.7	–	214 h	6 h 20 min
47.4	–	–	48 h 49 min

Furthermore, accuracy on the surface fields is met for different norms.

Relative $\|\cdot\|_2$ *and* $\|\cdot\|_\infty$ *errors*

	CFIE		CFIE + FMM		CFIE + OSRC + FMM	
k	$\|\cdot\|_2$	$\|\cdot\|_\infty$	$\|\cdot\|_2$	$\|\cdot\|_\infty$	$\|\cdot\|_2$	$\|\cdot\|_\infty$
4.76	6.3e-3	7.9e-3	5.5e-3	6.7e-3	6.8e-3	8.2e-3
11.85	2.5e-3	2.9e-3	3.9e-3	4.9e-3	2.2e-3	2.3e-3
23.7	–	–	1.67e-2	2.07e-2	2.02e-2	9.3e-3
47.4	–	–	–	–	2.46e-2	4.21e-2

The second example presented on Figure 15 consists in scattering by the cube with side lengths 2 and centered at the origin. We present two examples for two frequencies and adapted meshes.

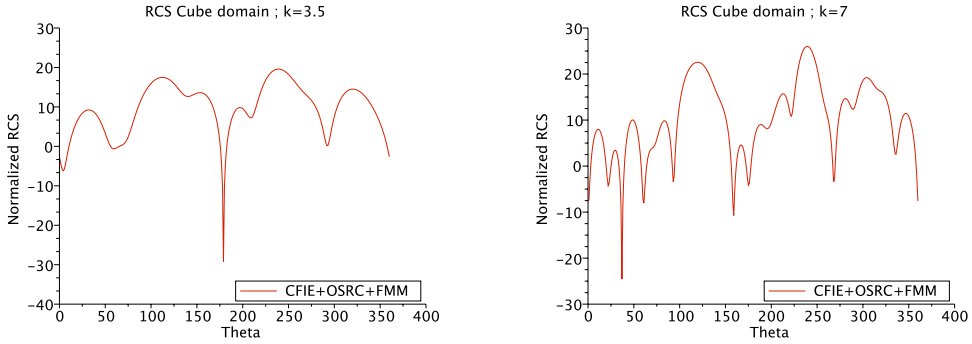

a) 4128 triangles b) 16930 triangles

Figure 15: Scattering by the cube $[-1,1]^3$, for $\boldsymbol{\theta}^{\text{inc}} = (\sqrt{3}/2, 0, 1/2)$

Finally, the last example (Figure 16) provides the RCS for scattering by a cube with a reentrant cavity which therefore is trapping. We can see that the RCS has a very complex structure which can be only accurately obtained by an accurate and efficient advanced numerical method like the integral equation formulations. Let us remark here that the mesh has been obtained by the freely available online mesh generator `Gmsh` which allows powerful features concerning two- and three-dimensional surface and volume meshes construction.

6 Conclusion

This course presented the basic notions and first implementations of integral equations in the time harmonic regime for acoustic scattering. Challenging questions nowadays are related to the high frequency regime where the wavelength λ is very small compared to the size of the scatterer. Let us mention that these equations are then solved by Fast Multilevel Multipole Methods which accelerate the matrix-vector products

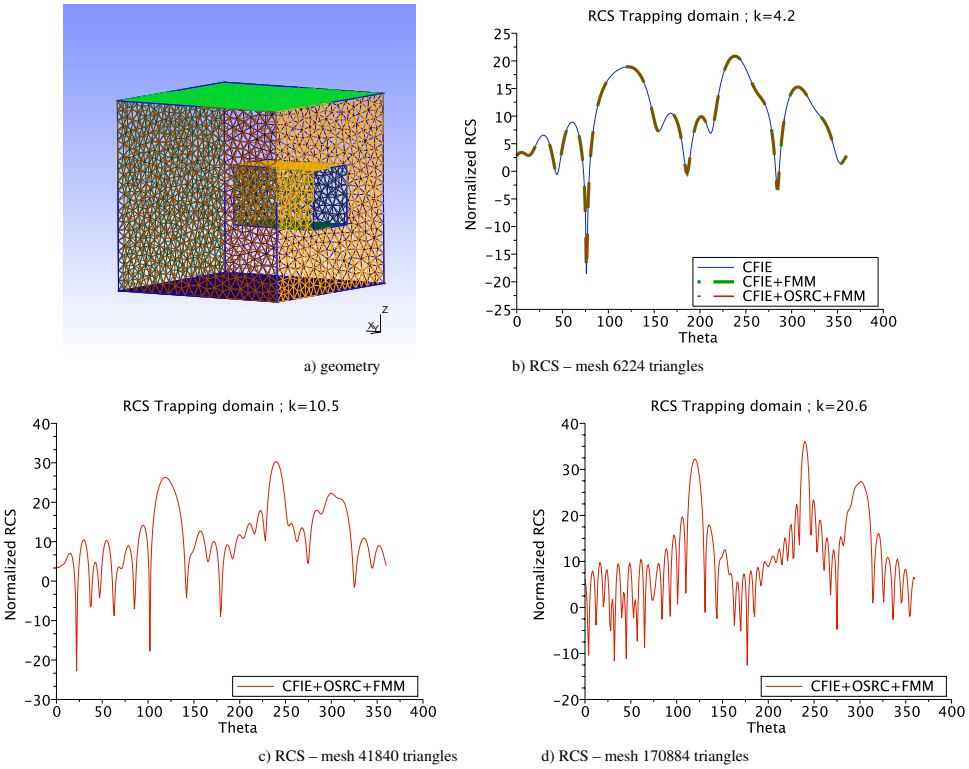

a) geometry

b) RCS – mesh 6224 triangles

c) RCS – mesh 41840 triangles

d) RCS – mesh 170884 triangles

Figure 16: Scattering by a cube with reentrant structure, for $\boldsymbol{\theta}^{\text{inc}} = (\sqrt{3}/2, 0, 1/2)$

and reduced the memory storage, in conjunction with preconditioned Krylov solvers. Other questions of interest are the case of penetrable bodies, coupling procedures with finite element methods when the obstacles are inhomogeneous, multiple scattering... Finally, most of the developments have extensions for vectorial Maxwell's equations for Maxwell's or elasticity equations. This is however very technical and out of the scope of this introductory course.

7 Acknowledgements.

The author is supported partially by the French ANR fundings under the project MicroWave NT09_460489 (http://microwave.math.cnrs.fr/). I also wish to thank M. Darbas, E. Darrigrand and Y. Lafranche for providing the three-dimensional numerical examples.

And last but not least, I wish to thank all the colleagues from the department of Mathematics of Simon Bolivar University (Caracas) and the students who attended the CIMPA school for the nice time spent there, discussing about numerics, mathematics and sharing ideas in a great place.

References

[1] M. Abramowitz and I.A. Stegun, Handbook of Mathematical Functions, Dover, New York, (1974).

[2] S. Amini, On the choice of the coupling parameter in boundary integral formulations of the exterior acoustic problem, Appl. Anal. **35** (1-4), (1990), pp.75-92.

[3] S. Amini and S.M. Kirkup, Solution of Helmholtz equation in exterior domain by elementary boundary integral equations, J. Comput. Phys. **118** (1995), pp. 208-221.

[4] X. Antoine, Conditions de Radiation sur le Bord, Ph.D. Thesis, University of Pau, 1997.

[5] X. Antoine, Fast approximate computation of a time-harmonic scattered field using the On-Surface Radiation Condition method, IMA J. Appl. Math. **66** (2001), pp. 83-110.

[6] X. Antoine, Advances in the On-Surface Radiation Condition Method: Theory, Numerics and Applications, Book Chapter in Computational Methods for Acoustics Problems, Editor F. Magoulès, Saxe-Coburg Publications, 2008, pp.169-194 (ISBN: 978-1-874672-30-2).

[7] X. Antoine, A. Bendali and M. Darbas, Analytic Preconditioners for the Electric Field Integral Equation, Int. J. Numer. Meth. Eng. **61** (2004), pp. 1310-1331.

[8] X. Antoine, A. Bendali and M. Darbas, Analytic Preconditioners for the Boundary Integral Solution of the Scattering of Acoustic Waves by Open Surfaces, J. Comput. Acoust. **13** (3), (2005), pp. 477-498.

[9] X. Antoine and Y. Boubendir, An integral preconditioner for solving the two-dimensional scattering transmission problem using integral equations, Int. J. Comput. Math., **85** (10), (2008), pp.1473-1490.

[10] X. Antoine and M. Darbas, Alternative integral equations for the iterative solution of acoustic scattering problems, Quarterly J. Mech. Appl. Math. **58** (2005), pp. 107-128.

[11] X. Antoine and M. Darbas, Generalized combined field integral equations for the iterative solution of the three-dimensional Helmholtz equation, Math. Model. Numer. Anal., **41** (1), (2007), pp.147-167.

[12] X. Antoine, C. Geuzaine and K. Ramdani, Computational Methods for Multiple Scattering at High Frequency with Applications to Periodic Structures Calculations, M. Ehrhardt (Ed.), Wave Propagation in Periodic Media - Analysis, Numerical Techniques and Practical Applications, Progress in Computational Physics, Vol. 1, Bentham Science Publishers Ltd., 2009.

[13] H. Brakhage and P. Werner, Über das Dirichletsche Aussenraumproblem für die Helmholtzsche Schwingungsgleichung, Numer. Math., **16**, (1965), pp.325–329.

[14] O.P. Bruno, T. Elling, and C. Turc, Well conditioned high-order algorithms for the solution of three-dimensional surface acoustic scattering problems with Neumann boundary conditions, submitted, 2009.

[15] O. Bruno and C. Geuzaine, An $\mathcal{O}(1)$ integration scheme for three-dimensional

surface scattering problems, J. Comput. Appl. Math., **204**, (2007), pp.463–476.
[16] O. Bruno, C. Geuzaine, J. Monro, Jr., and F. Reitich, Prescribed error tolerances within fixed computational times for scattering problems of arbitrarily high frequency: the convex case, Philosophical Transactions of the Royal Society (Series A: Mathematical, Physical and Engineering Sciences), **362** (1816), (2004), pp.629-645.
[17] O.P. Bruno and L.A. Kunyansky, High-order algorithm for the solution of surface scattering problems: Basic implementation, tests, and applications, J. Comput. Phys. **169**, (2001), pp.80–110.
[18] A. Buffa and R. Hiptmair, Regularized combined field integral equations, Numer. Math., **100** (1), (2005), pp.1-19.
[19] A. J. Burton and G. F. Miller, The application of integral equation methods to the numerical solution of some exterior boundary-value problems, Proc. Roy. Soc. London. Ser. A, **323**, (1971), pp.201-210.
[20] B. Carpentieri, I. S. Duff, and L. Giraud, Sparse pattern selection strategies for robust Frobenius-norm minimization preconditioners in electromagnetics, Numer. Linear Algebra Appl. 7 (2000), pp. 667-685.
[21] B. Carpentieri, I. S. Duff and L. Giraud, Experiments with sparse approximate preconditioning of dense linear problems form electromagnetic applications, Tech. Rep. TR/PA/00/04, CERFACS, France, (2000).
[22] S.N. Chandler-Wilde, I.G. Graham, S. Langdon and M. Lindner, Condition number estimates for combined potential boundary integral operators in acoustic scattering, J. Int. Eq. Appl. **21** (2) (2009), pp.229-279.
[23] W.C. Chew, J.M. Jin, E. Michielssen and J. Song, "Fast and Efficient Algorithms in Computational Electromagnetics", Artech House Antennas and Propagation Library, Norwood, 2001.
[24] S.H. Christiansen, Résolution des équations intégrales pour la diffraction d'ondes acoustiques et électromagnétiques. Stabilisation d'algorithmes itératifs et aspects de l'analyse numérique, PhD Thesis, Ecole Polytechnique, Palaiseau, France, (2001).
[25] P.G. Ciarlet, "Introduction à l'analyse numérique matricielle et à l'optimisation", Masson, Paris, 1982.
[26] R. Coifman, V. Rokhlin and S. Wandzura, "The Fast Multipole Method for the wave equation: A pedestrian description", IEEE Trans. on Ant. and Prop., **35**(3), (1993), pp.7-12.
[27] D. L. Colton and R. Kress, "Integral equation methods in scattering theory", Pure and Applied Mathematics, John Wiley and Sons Inc., 1983.
[28] M. Costabel, Integral equation methods in scattering theory, SIAM J. Math. Anal. **19**, (1988), pp.613-626.
[29] M. Darbas, Préconditionneurs analytiques de type Calderon pour les formulations intégrales des problèmes de diffraction d'ondes,, PhD Thesis, Toulouse, 2004.
[30] E. Darrigrand, Couplage Méthodes Multipôles Rapides et Discrétisation Microlocale pour les Equations Intégrales de l'Electromagnétisme, PhD Thesis,

Bordeaux, 2002.
[31] E. Darve, Méthodes multipôles rapides: Résolution des équations de Maxwell par formulations intégrales, Ph.D. Thesis, Paris 6, 1999.
[32] A. Greenbaum, Iterative Methods for Solving Linear Systems, Frontiers in Applied Mathematics, **27**, Society for Industrial and Applied Mathematics (SIAM), Philadelphia, PA, 1997.
[33] L. Greengard and V. Rokhlin, A fast algorithm for particle simulations, J. Comput. Phys., **73** (2), (1987), pp.325-348.
[34] R. Kerchroud, A. Soulaimani and X. Antoine, Performance study of plane wave finite element methods with a Padé-type artificial boundary condition in acoustic scattering, Adv. Eng. Soft. **40** (2009), pp. 738-750.
[35] R. Kerchroud, A. Soulaimani and Y. Saad, Preconditioning techniques for the solution of the Helmholtz equation by the finite element method, Math. Comput. Simul., **65** (4-5), (2004), pp.303-321.
[36] R. Kress, Minimizing the condition number of boundary integral operators in acoustic and electromagnetic scattering, Quart. J. Mech. Appl. Math., **38** (2), (1985), pp.323-341.
[37] R. Kress, Linear Integral Equations, Second Ed., Applied Mathematical Sciences (82), New York, Springer-Verlag, 1999.
[38] R. Kress and W. T. Spassov, On the condition number of boundary integral operators for the exterior Dirichlet problem for the Helmholtz equation, Numer. Math., **42** (1), (1983), pp.77-95.
[39] G.A. Kriegsmann, A. Taflove and K.R. Umashankar, A new formulation of electromagnetic wave scattering using the on-surface radiation condition method, IEEE Trans. Antennas Propag. **35** (1987), pp. 153-161.
[40] S. Lang, Linear Algebra, Springer, 3rd edition, 2004.
[41] W. McLean, Strongly Elliptic Systems and Boundary Integral Equations, Cambridge University Press, Cambridge, 2000.
[42] D. P. Levadoux, Etude d'une Equation Intégrale Adaptée à la Résolution Hautes Fréquences de l'Equation de Helmholtz, PhD thesis, Université Paris VI, 2001.
[43] J.-C. Nédélec, Acoustic and Electromagnetic Equations, Applied Mathematical Sciences (144), New York, Springer-Verlag, 2001.
[44] D. Osei-Kuffuor and Y. Saad, Preconditioning Helmholtz linear systems, Applied Numerical Mathematics (in press, 2010).
[45] V. Rokhlin, Rapid solution of integral equations of scattering theory in two dimensions, J. Comput. Phys. **86** (2) (1990), pp. 414-439.
[46] Y. Saad, Iterative Methods for Sparse Linear Systems", PWS Publishing Company, Boston, 1996.
[47] Y. Saad and M.H. Schultz, A generalized minimal residual algorithm for solving nonsymmetric linear systems, SIAM J. Sci. Comput., **7** (3), (1986), pp.856-869.
[48] L. Schwartz, Théorie des Distributions, Broché, 1997.
[49] O. Steinbach and W. L. Wendland, The construction of some efficient preconditioners in the boundary element method, Adv. Comput. Math. **9** (1-2) (1998), pp. 191-216.

[50] G. Sylvand, La Méthode Multipôle Rapide en Electromagnétisme: Performances, Parallélisation, Applications", Thèse de Doctorat, ENPC, 2002.

[51] M.E. Taylor, Pseudodifferential Operators, Princeton Mathematical Series, 34, Princeton University Press, 1981, xi+452.

[52] L.L. Thompson, A review of finite-element methods for time-harmonic acoustics, J. Acoust. Soc. Amer., **119** (3), (2006), pp. 2272-2293.

[53] L. N. Trefethen, Pseudospectra of Matrices, editors D. F. Griffiths, G. A. Watson., in "Numerical Analysis", Longman Scientific and Technical, 1991.

[54] E. Turkel, Boundary Conditions and Iterative Schemes for the Helmholtz Equation in Unbounded Regions, Book Chapter in Computational Methods for Acoustics Problems, Editor F. Magoulès, Saxe-Coburg Publications, 2008, pp. 127-159 (ISBN: 978-1-874672-30-2).

[55] Y. Wang, J. Lee and J. Zhang, A short survey on preconditioning techniques for large-scale dense complex linear systems in electromagnetics, Int. J. Comp. Math. **84** (8) (2007), pp. 1211-1223.